<Review Article>Heat Flow in Particle Mat and Properties of Particleboard under Steam-Injection Pressing

AUTHOR(S):

HATA, Toshimitsu

CITATION:

HATA, Toshimitsu. <Review Article>Heat Flow in Particle Mat and Properties of Particleboard under Steam-Injection Pressing. Wood research : bulletin of the Wood Research Institute Kyoto University 1993, 80: 1-47

ISSUE DATE:

1993-11-30

URL:

http://hdl.handle.net/2433/53256

Review Article

Heat Flow in Particle Mat and Properties of Particleboard under Steam-Injection Pressing*

Toshimitsu HATA**

(Received August 30, 1993)

Keywords: steam-injection pressing, temperature behavior, particle geometry, gas permeability, board properties

Contents

Introduction
Chapter 1 Heat Flow in Particle Mat During Pressing
1.1 Temperature behavior in particle mat during hotpressing and steam-injection pressing
1.1.1 Experimental
1.1.2 Results and discussion
Conventional hotpressing
Steam-injection pressing
1.2 Computer simulation of temperature behavior in particle mat during steam-injection pressing
1.2.1 Theory for the prediction of temperature behavior in mat
1.2.2 Input data for the calculation of temperature behavior
1.2.3 Numerical procedure
1.2.4 Results and discussion
1.3 Summary
Chapter 2 Steam Diffusion in Particle Mat During Steam-Injection Pressing
2.1 Effects of particle geometry on temperature behaviors in particle mats
2.1.1 Experimental
Regulation of particles
Temperature behaviors in mats
2.1.2 Results and discussion

* This review article is the abstract of the doctor thesis by the author (Kyoto University, 1993).

** Laboratory of Wood Composite.

2.2 Effects of particle geometry on the gas permeabilities of boards
2.2.1 Experimental
Measurements of air permeabilities of boards
2.2.2 Results and discussion
Air permeabilities of boards
Multiple regression analysis
2.3 Summary
Chapter 3 Physical and Mechanical Properties of Particleboard Produced by Steam-Injection Pressing
3.1 Effects of steam-injection time and timing on board properties
3.1.1 Experimental
3.1.2 Results and discussion
Effect of steam-injection time
Effect of steam-injection timing
3.2 Effect of particle geometry on board properties
3.2.1 Experimental
3.2.2 Results and discussion
3.3 Shortening press cycle with steam-injection pressing
3.3.1 Experimental
3.3.2 Results and discussion
3.4 Summary
Conclusion
Acknowledgement
References

Introduction[1)]

In the production of particleboard, the pressing process is the most important for both productivity and board quality. For that reason, efforts are being made to develop the new methods of pressing technology and new types of resin[2,3)].

The efforts for the former were crowned with successfully developing a multi-opening press, single-opening press and continuous press[4–8)], which are based on a hotpressing. On the contrary, a steam-injection pressing in which high pressure steam is injected into a mat during pressing have awakened a world interest recently. The mechanism of heat transfer in mats during steam-injection pressing is different from that in the conventional hotpressing. In the former, a high-pressure steam flow governs the heat transfer through particle mat, while in the latter the hot-platens supply heat energy to the mat by heat conduction. In this regard, the steam-injection pressing is expected to have the advantage of shortening the total pressing time than the conventional hotpressing.

Studies on isocyanate bonded particleboard have been conducted in an effort to develop new types of resin[9–11]. In Japan many studies on low-density particleboard with a density of about 0.4 g/cm^3 have been done in order to substitute particleboard for plywood. Low-density particleboards bonded with an isocyanate compound adhesive suitable for both exterior and interior uses have been reported[3,12–14]. The features of the isocyanate compound resins are as follows: 1) hot pressing time can be shortened as the adhesive reactivity is higher; and 2) the allowable range of moisture is broader.

The remarkable features of the low-density board include high dimensional stability and internal bond strength in spite of its lower density, although the flexural properties are rather poor. The simple way to improve the flexure property is to increase the board thickness. However, the pressing time increases in direct proportion to the board thicknesses in the conventional hotpressing, thus the production efficiency is decreased.

The purpose of the present study is to establish the technology for the steam-injection pressing process and to apply this technology in the production of thick low-density particleboard. The present paper consists of four chapters;

Chapter 1 : The temperature behavior in particle mats during hotpressing and steam-injection pressing;

Chapter 2 : The effect of particle geometry on the temperature behavior in particle mat and on the gas permeabilities in the particleboard;

Chapter 3 : The effects of injection time and timing, and particle geometry on the board properties, and the trial of shortening the press cycle with steam-injection.

Chapter 1 Heat Flow in Particle Mat During Pressing

The temperature behavior which is the most fundamental information to decide optimum conditions during pressing is examined. The theory for heat conduction in wood was discussed by Maku[15,16]. This theory which was analytically applied to wood drying can also be applied to calculate the temperature distribution in a particle mat during conventional hotpressing. Heat transfer in a mat during hotpressing accompanying steam injection, however, has not been discussed yet. The thermal flow in a dry particle mat is theoretically discussed for both pressings, and the theoretical equations proposed are examined by use of experimental data in this chapter. The core temperature curves during pressing can be simulated by means of a computer under various conditions according to the obtained equations.

1.1 Temperature behavior in particle mat during hotpressing and steam-injection pressing[17]

1.1.1 Experimental

Flake-type particles of seraya (Shorea spp.) 13 mm long, 1.6 mm wide and 0.6 mm thick

on the average were prepared. Upper and lower hot platens were regulated at the same temperature of 160°C, and for convenience no binders were applied to the particles.

The temperature distribution along the mat thickness was measured by means of Copper-Constantan thermocouples with wire diameters of 0.2 mm, inserted into the center of the mat plane at different layers. These were connected to a data processor via a data-logger, and the temperature at each point was recorded at certain time intervals. In a preliminary experiment, the temperature distribution at each layer of the mat was uniform during hot-pressing. Figure 1.1 shows the measuring points along the mat thickness. The error was estimated at ±0.5°C.

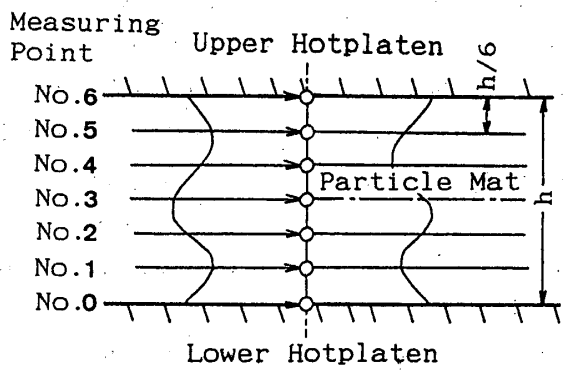

Fig. 1.1. Measuring points of temperature of mats during hot-pressing and steam-injection pressing.

The measurement started at the moment when pressure was applied to a particle mat. In hotpressing, the target mat densities were 0.4 and 0.6 g/cm^3 at thicknesses of 20, 30 and 40 mm, which was controlled by distance bars inserted on both sides of the mat in the press. The effect of moisture content on the temperature distribution was examined by use of particles with different moisture contents and by use of wetted papers covering the top and bottom of the mat so that the moisture content in the face layers is higher than that of the inner layers. This method

Table 1.1. The factors and levels taken in the experiment on hot-pressing.

Parameters	Measurement of temperature distribution within a layer	Measurement of the temperature at the center of the layers	
		Uniformly distributed moisture content	Higher moisture contemt in mat surface
Mat thickness (mm)	20, 40	20, 30, 40	20, 30, 40
Mat density (g/cm^3)	0.4, 0.6	0.4, 0.6	0.4, 0.6
Particle m.c.* (%)	10.1	0, 11, 30	0
Equivalent m.c. of wet paper (%)			20, 26, 31, 35

* Moisture content in the wet papers covered the both surfaces of mat is expressed as the equivalent moisture content which would be calculated on whole particle mat if the moisture would distributre uniformly in the mat.

shortens the pressing time due to the fast heat transfer by the steam evaporated from the mat surfaces to the core, thus the same effect as that of steam-injection pressing can be expected. The factors and levels taken in the hotpressing experiment are summarized in Table 1.1.

For steam-injection pressing, a set of 600×600×30 mm perforated plates for steam-injection were prepared to fit the surfaces of the hotplatens of the conventional laboratory hotpress. The upper and lower plates were perforated with 2 mm-diameter holes drilled through half the depth of the plates with a 25×25 mm spacing pattern, which covered an area of 450×375 mm for the upper plate and of 475×400 mm for the lower plate. The holes on the upper platen and those on the lower platen were drilled in staggered position relative to each other. A vapor seal on the edge of the mat as reported by Shen[18] was not used.

Thirty seconds into pressing time, or after the press pressure had begun to build up, high pressure steam was injected. The steam-injection periods were 3, 10, 30 and 120 s. Adjusted initial steam pressures were 6.2 and 10.0 kgf/cm^2 corresponding to 160 and 180°C, respectively. However, the effective steam pressure during the injection was reduced to some extent. In mats with a density of 0.4 g/cm^3, the effective steam pressure were 4 and 6 kgf/cm^2, when the initial pressures were set at 6.2 and 10.0 kgf/cm^2, respectively, while the effective steam pressure was 5.5 kgf/cm^2 for a mat with a density of 0.6 g/cm^3 at the initial steam pressure of 6.2 kgf/cm^2. The target air-dry densities of the mats were 0.4 and 0.6 g/cm^3 and target thicknesses were 20 and 40 mm.

The factors and levels taken in the experiment on steam-injection pressing are summarized in Table 1.2.

Table. 1.2. The factors and levels taken in the standard of the experiment on steam-injection pressing.

Parameters	Measurement in the horizontal plane	Measurement in the thickness direction
Mat thickness (mm)	20	20, 40
Mat density (g/cm^3)	0.4	0.4, 0.6
Particle m.c. (%)	10.1	0.4, 11
Injection time (sec)	30	3, 10, 30, 120
Vapor pressure (kgf/cm^3)	6.3	6.3, 10.2

1.1.2 Results and discussion

The temperature distribution in the middle layer of the mat during hotpressing was as uniform as that in hotplatens (coefficient of variation 1.6%). A more uniform distribution which was independent of the location of steam perforations was observed in steam-injection pressing. Therefore, in the present paper only the temperature behavior through the mat thickness at the center of mat plane is discussed.

Figure 1.2 shows a typical example of temperatures in different layers of the particle mat as a

function of time during hotpressing and steam-injection pressing. Because of the seasonal changes of temperature, the initial mat temperature in the case of hotpressing is slightly different from that of steam-injection pressing. The temperatures of all the mat layers increased to more than 100°C almost immediately after the start of steam-injection. As soon as steam is injected, vapor diffuses through the mat with the driving force of steam pressure gradient. On the other hand, the temperature increase in the mat during hotpressing depends very much on the position within the mat. The core temperature increases slowly and requires about 11–11.5 min for a mat of 40 mm thickness to reach 100°C. The press time of a low density particleboard of 40 mm thickness bonded with an isocyanate compound adhesive is taken to be 12 min at a platen temperature of 160°C[13]. It took about 1 min to cure the resin in the middle layer of the mat after the temperature of the layer had reached 100°C. Therefore, in steam-injection pressing can it be predicted to shorten the pressing time to 1/10 (for a board of 40 mm in thickness) of that of conventional hotpressing.

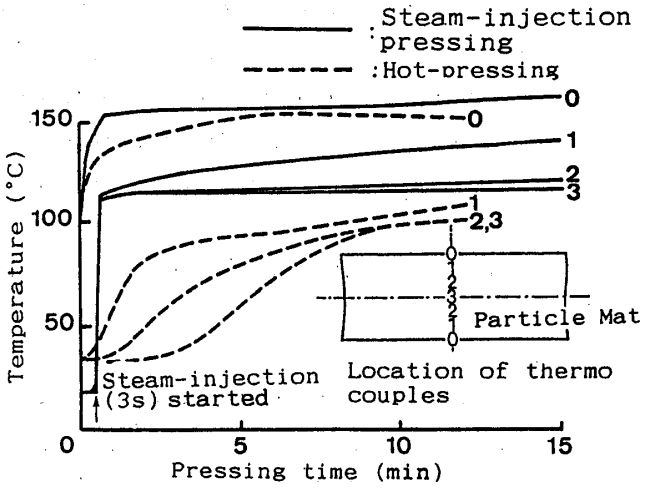

Fig. 1.2. Temperature behavior of mat during hot-pressing and steam-injection pressing.
Note: mat density=0.4 g/cm^3, mat thickness=40 mm, moisture content of mat before pressing 0% (steam-injection pressing), 11% (hot-pressing).

Conventional hotpressing

The core temperature of particle mats with different densities and moisture contents are shown in Figs. 1.3–1.5 as a function of elapsed time.

Figure 1.3 shows the core temperature of mats with a different density and thickness at a moisture content of 11% as a function of time. With the increase of the mat thickness from 20 to 40 mm, the slope of the temperature curve decreased. It was calculated that it takes about 3 and 11 min for the core temperatures of mats with a thickness of 20 and 40 mm, respectively, to reach 100°C. According to the heat conduction theory, when the thickness of the mat is doubled, the time required to increase core temperature to a certain level should increase four times. The

experimental result shows that the temperature behavior of particle mat with low moisture content in hotpressing obeys principally the heat conduction law.

The effect of mat density on the temperature increase with passage of time is very slight, as shown in Figure 1.3. However as the density increased, the rate of temperature increase seems to decrease due to the increase of heat capacity per unit volume of mat.

Figure 1.4 shows the effect of the initial moisture content of the particles on the core temperature of the mats as a function of time. The density and the thickness of the mat were 0.4 g/cm^3 and 30 mm, respectively. From the figure, the following can be observed ; the higher the moisture content is, the shorter is the time necessary for the core of mat to reach 100°C, while the time to stay at a constant temperature about 100°C is longer. It has been confirmed that the core temperature begins to rise again from 100°C as the particles lose moisture below 10% moisture

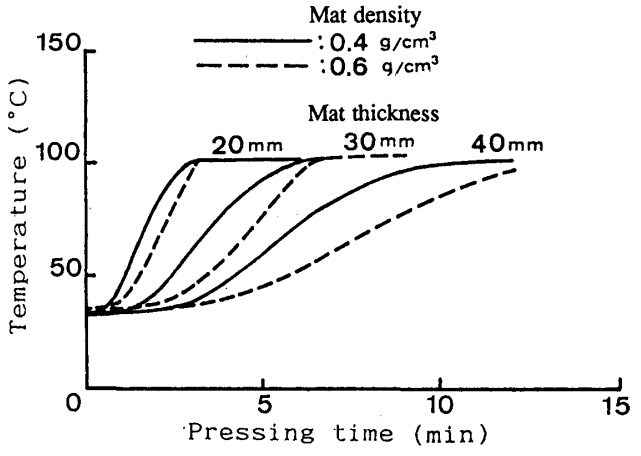

Fig. 1.3. The effect of mat density and thickness on the core temperature of mats as a function of time during hot-pressing.
Note: Mat moisture content before pressing=11%.

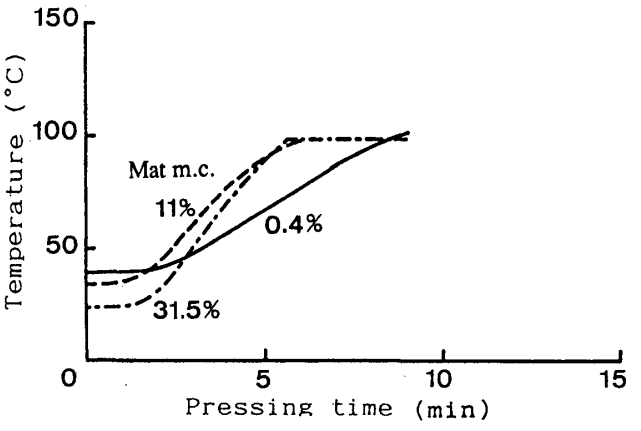

Fig. 1.4. The effect of moisture content of mat before pressing on the core temperature of mats along the thickness as a function of time during hot-pressing.
Note: Mat thickness=30 mm, Mat density=0.4 g/cm^3.

content[19,20]. When dry particles are used, no equilibrium state of temperature at 100°C is observed.

Figure 1.5 shows the core temperature of dry mats covered on both surfaces with wet papers. The basis weight of the paper was 80 g/m^2. In the figure, moisture contained in the wet papers is expressed as an equivalent moisture content which would be calculated on the whole particle mat if the moisture were distributed uniformly in the mat. When both the face and the back of the mat have a higher moisture content, the increase of mat thickness from 20 to 40 mm does not affect the time required for the core temperature to reach 100°C and the rate of increase is much higher than without wet papers. Comparing Figure 1.5 with Figure 1.4, the rate of increase of the temperature of mat overlaid with wet papers shows more than four times as much as that of a mat which has a uniform moisture distribution. It is noteworthy that the temperature in the middle layer rose to more than 100°C when the equivalent moisture content of wet paper was more than 30%, while it remained at 100°C for mats having less than 30% equivalent moisture content. This suggests that the water vapor moving toward the middle layer of the mat exceeds the vapor moving out of this layer when enough water exists at the surface, and the sorption heat of water on particles may promote the temperature increase in the core, so that internal vapor pressure increases.

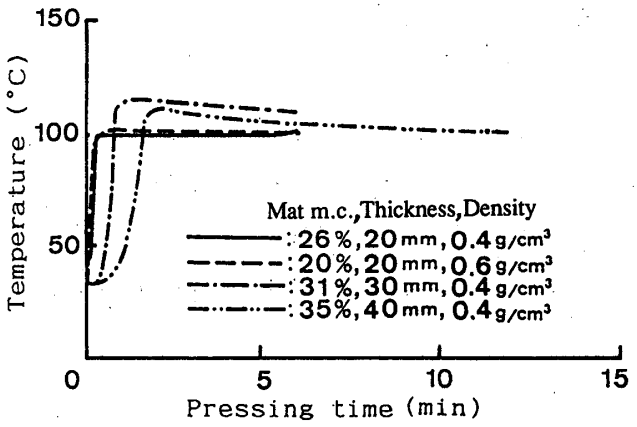

Fig. 1.5. The core temperature of mats with wet paper overlays.
Note: Particle moisture content=0%, e.m.c.=equivalent moisture content which expresses the moisture contained in the wet papers as if distributed uniformly in the wholemat.

Steam-injection pressing

During steam-injection, the variation of temperature within the plane of the middle layer of mat was less than in the conventional hotpressing.

Figure 1.6 shows the effect of steam-injection time on the core temperature of the mat. The target density and the mat thickness were 0.4 g/cm^3 and 20 mm, respectively. Dry particles (0% moisture content) were used for this series of experiments. When steam was injected for a longer time, the core mat temperature was kept constant during injection. This suggests that with the

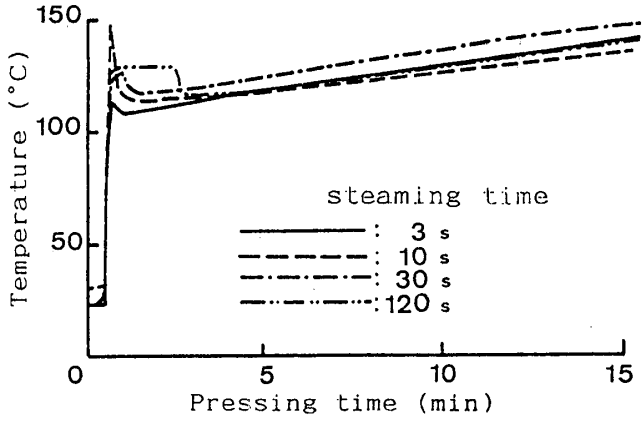

Fig. 1.6. The effect of steam-injection time on the core temperature of mats.
Note: Mat density=0.4 g/cm^3, mat thickness=20 mm, moisture content=0%, effective steam pressure=4 kgf/cm^2.

increase of the steam-injection time the inflow and outflow of steam in the middle layer of mat was kept balance, and the inner vapor pressure maintained constant. After injection was stopped, the inner vapor pressure or the temperature of the middle layer falls down due to the outflow of steam from edges of mat. However, the temperature goes down once, then increases gradually again, and the increasing curves with different injecting time show almost similar figure, which is quite different from that in the case of mats with wet paper overlay. This suggests that steam-injection up to 120 s does not increase moisture content of the middle layer of mat to more than 10%[19,20]. This result agrees with those obtained by Geimer[2] and Shen[18].

Figure 1.7 shows the effects of mat thickness and moisture content on the core temperature of mats with density of 0.4 g/cm^3 during steam-injection pressing. The core temperature of a mat with a thickness of 40 mm immediately rises to more than 100°C in the same way as that of a mat with a 20 mm thickness during steam-injection in the range of steam pressures used in this

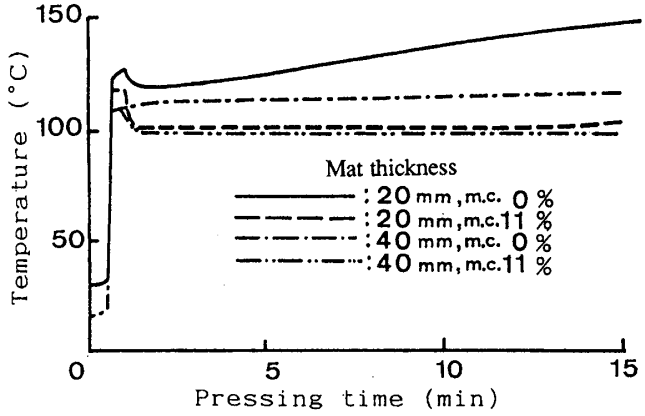

Fig. 1.7. The effect of mat thickness and moisture content on the core temperature of mats during steam-injection pressing.
Note: Injection time=30 sec, mat density=0.4 g/cm^3

experiment. However, the maximum temperature reached at the middle layer during steam-injection showed a tendency to decrease with an increase of the mat thickness. The temperature curves after stopping the steam-injection were greatly affected by the mat thickness, which depends greatly on heat conduction from the hot platens.

When steam is injected, the temperature curves of air-dry (11%) particle mat are similar to those of dry mats, and seem to be independent of the moisture content. This suggests that most of the steam injected does not interact with the moisture present in the particles and diffuses through the particles from the hot-platens to the middle mat layer. However, the temperature of the middle layer of air-dry mats decreases to 100°C after stopping the steam-injection and then increases gradually at a rate lower than that of the dry-mat, because the heat energy supplied from the hot-platens is partly consumed for evaporation of water present in the particles.

Figure 1.8 shows the core temperature of mats with a density of 0.6 g/cm^3 under different conditions of moisture content and steam-injection time. When steam is injected, the core of a

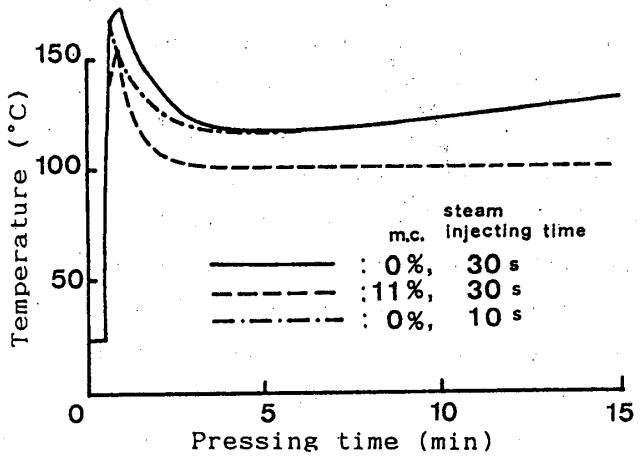

Fig. 1.8. The core temperature of mats during steam-injection pressing.
Note: Mat thickness=20 mm, mat density=0.6 g/cm^3.

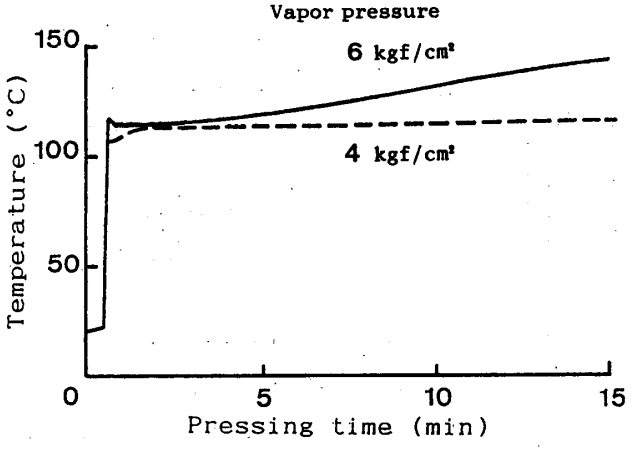

Fig. 1.9. The core temperature of mats during steam-injection pressing.
Note: Mat thickness=20 mm, mat density=0.4 g/cm^3

mat with a density of 0.6 g/cm^3 reaches a higher temperature than that of a mat with the density of 0.4 g/cm^3. With increasing density, the gaps among the particles which are considered to be the main paths of the steam become narrower. This means that the resistance to the diffusion of vapor in the mat becomes greater with increasing mat density. On the other hand, resistance to the outflow from the edges of mat also increases. Therefore, when the supply of steam is sufficient, the inflow and outflow of steam in mat balances at a higher vapor pressure, and the core mat temperature reaches a higher level.

When steam with higher pressure is injected, the core temperature rises to a higher level than that with lower pressure as shown in Figure 1.9.

1.2 Computer simulation of temperature behavior in particle mat during steam-injection pressing[21,22)]

1.2.1 Theory for the prediction of temperature behavior in mat

During steam-injection and period following the injection, the mat temperature increase is mainly caused by the high temperature steam moving among particles through the mat. The steam movement is presumed to be a diffusion phenomenon based on vapor pressure gradient as a driving force. The equation for the diffusion analysis is similar to that of heat conduction. Therefore the finite element equation applied for the heat conduction analysis would also be applicable.

In general, mass flow in a porous matrix is controlled by many driving forces. When these forces are treated as a potential gradient of a whole, the mass flow is expressed as follows:

$$\text{flux} = Q/A = k(\partial\phi/\partial x), \tag{1}$$

where Q/A is a mass flow [g·s^{-1}·cm^{-2}], k is a proportional coefficient [g·cm^{-1}·atm^{-1}·s^{-1}], $\partial\phi/\partial x$ is a potential gradient which is expressed as follows:

$$\partial\phi/\partial x = \partial(P_1 + P_+ P_3 + \ldots)/\partial x. \tag{2}$$

The driving forces, shown at the right of Eq. (2), are given the gradients of external pressure potential, pneumatic potential, osmotic potential, gravitational potential, and so on[23)].

As in the case of steam-injection pressing where steam is injected into a particle mat, the external pressure gradient, (dP_1/dx), and the concentration gradient, (dP_2/dx), can be given as the main potential gradient $(\partial\phi/\partial x)$. Therefore, Eq. (1) becomes

$$\text{flux} = -k_1 dP_1/k_2 dP_2/dx. \tag{3}$$

The first and second terms of the right of Eq. (3) correspond to Darcy's law for gases and Fick's law of diffusion, respectively, and k_1 and k_2 of the potential coefficients are called as gas permeability and diffusion coefficient, respectively.

When the interaction of adsorption and desorption on wood by steam is ignored, and the gas transportation such as air through the pores among particles in a mat is assumed, the first term of Eq. (3) mainly controls the flux because k_1 is greater than k_2 during steam-injection. On the other hand, after stopping the steam-injection, the external steam pressure gradient dP_1/dx

becomes zero, and the second term of Eq. (3) controls the flux. As the concentration, the pressure, and the temperature of saturated steam are considered to be functions of each other, the driving force, dP_2/dx, can be expressed as a pressure gradient.

Therefore, steam transported through mats during steam-injection pressing is approximated with the following equation:

$$\text{flux} = -kdP/dx \tag{4}$$

Comparing this equation with Eq. (3), the right term of Eq. (4) corresponds to $k_1(dP_1/dx)$ during steam-injection and to $k_2(dP_2/dx)$ after the injection of steam.

By using the continuous equation, the unsteady state diffusion equation is derived from Eq. (4) as

$$\frac{\partial}{\partial t}\rho_s = \frac{\partial}{\partial x_i}\left(k\frac{\partial P}{\partial x_i}\right) \tag{5}$$

where, ρ_s is a steam density [g·cm^{-3}].

When the interaction between steam and particles is neglected, the gradient of the saturated steam pressure P to steam density ρ_s is constant. Using the gradient of the steam mass density ρ_s/x_i [g·cm^{-4}], Eq. (5) can be expressed as

$$\frac{\partial \rho_s}{\partial t} = \frac{\partial}{\partial x_i}\left(k_\rho \frac{\partial \rho_s}{\partial x_i}\right) \tag{6}$$

where, $k_\rho = k(\partial P/\partial \rho_s)$ (7)

k_ρ is the gas permeability of a particle mat based on steam density gradient [cm·s^{-2}l].

When the diffusion coefficient is independent of the steam density, Eq. (6) is expressed as

$$\frac{\partial \rho_s}{\partial t} = k_{\rho x}\frac{\partial^2 \rho_s}{\partial x^2} + k_{\rho y}\frac{\partial^2 \rho_s}{\partial y^2} + k_{\rho z}\frac{\partial^2 \rho_s}{\partial x^2} \tag{8}$$

where, $k_{\rho x}$, $k_{\rho y}$, and $k_{\rho z}$ is a diffusion coefficient [cm^2·s^{-1}] of steam moving in the direction of the x, y and z axes, respectively.

If the diffusion coefficient is uniform in all directions and in every part of the mat, from Eq. (8), we obtain the equation,

$$\frac{\partial \rho_s}{\partial t} = k_\rho\left(\frac{\partial^2 \rho_s}{\partial x^2} + \frac{\partial^2 \rho_s}{\partial y^2} + \frac{\partial^2 \rho_s}{\partial z^2}\right) \tag{9}$$

where, k_ρ ($=k_{\rho x}=k_{\rho y}=k_{\rho z}$) is the diffusion coefficient of steam in a particle mat [cm^2·s^{-1}].

The steam density on the boundary between a mat surface and a hot-platen is defined as,

$$\rho_s = \bar{\rho}_s \tag{10}$$

where, $\bar{\rho}_s$ is the saturated steam density at a regulated vapor pressure [g·cm^{-3}].

The mass flux J_p of steam evaporation from mat sides [g·cm^{-2}·s^{-1}] is given as

$$J_p = k_p(p_w - p_0) \tag{11}$$

where, k_p is the surface evaporation coefficient [g·cm^{-2}·s^{-1}·mmHg^{-1}], p_w the steam pressure at the surface of the mat sides [mmHg], and p_0 the steam pressure in environmental air

[mmHg].

Eq. (11) can be expressed in terms of steam density as

$$J_p = k_\rho(\rho_w - \rho_0) \tag{12}$$

where, J_ρ is the steam flux [g·cm^{-2}·s^{-1}] corresponding to J_p, k_ρ the surface evaporation coefficient of steam based on the steam density gradient [cm·s^{-1}], and ρ_w, ρ_0 the steam densities in g·cm^{-3} corresponding to the steam pressures p_w and p_0, respectively.

The initial condition is expressed as

$$\rho(r, 0) = \Omega(r) \tag{13}$$

where, $\rho(r, 0)$ is the steam density at the position r and at the time 0, (r) is a known function.

The standard equation of the finite element method derived from Eq. (9) is expressed in the same way as that of conventional hotplaten pressing;

$$[K]\{\Psi\} + C]\{\partial\Psi/\partial t\} = \{F\} \tag{14}$$

where, $\{\Psi\}$ the grid point vapor density vector for the whole elements,

$$[K] = \sum_e \left\{ \int_{V^e} k_\rho \left(\frac{\partial[N]^T}{\partial x}\frac{\partial[N]}{\partial x} + \frac{\partial[N]^T}{\partial y}\frac{\partial[N]}{\partial y} + \frac{\partial[N]^T}{\partial z}\frac{\partial[N]}{\partial z} \right) dV + \int_{S^e} k_\rho [N]^T [N] dS \right\}, \tag{15}$$

$$[C] = \sum_e \left\{ \int_{V^e} [N]^T [N] dV \right\}, \tag{16}$$

and

$$[F] = \sum_e \left\{ \int_{S^e} k_\rho \rho_0 [N]^T dS \right\}, \tag{17}$$

Approximating the time term of Eq. (14) by the difference method, we obtain,

$$\left(\frac{1}{2}[K] + \frac{1}{\Delta t}[C] \right) \{\Psi(t+\Delta t)\} = \left(\frac{-1}{2}[K] + \frac{1}{\Delta t}[C] \right) \{\Psi(t)\} + \{F\} \tag{18}$$

When $\{\Psi\}$ is known, the equation of the finite element method for the unsteady state diffusion problem can be solved step by step using Eq. (18).

It was found from experimental measurements that the temperature distribution in mat

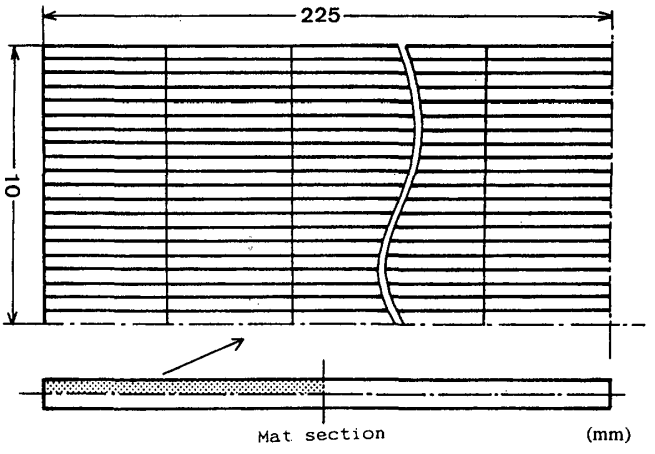

Fig. 1.10. Typical elements division (in the case of a 20 mm thick mat).

during hotpressing was symmetric with respect to the horizontal and vertical axes through the mat center. As shown in Figure 1.10 the mat section was divided into four parts by two axes, one of which was taken as the range for calculation. The range was divided by 20 (lengthwise) × 50 rectangular elements.

1.2.2 Input data for the calculation of temperature behavior

The particle geometry and the compaction ratio (board density/particle density) are the important factors that influence the steam diffusion in the mat[24,25]. The effect of particle geometry on the gas permeability of mats is to be discussed in the next section.

When the particle size is 13 mm long, 1.6 mm wide, and 0.6 mm thick as given in the experiment of section 1.1.1 and steam is injected at the compaction ratio of 1.0, k in the vertical direction to the platen is 5.68 $g \cdot cm^{-1} \cdot atm^{-1} \cdot s^{-1}$ [24]. As $\partial P/\partial \rho_s$ of saturated steam is 1,893 $g^{-1} \cdot cm^{-1} \cdot atm^{-1}$ from Eq. (7), k_ρ is calculated to be 10,753 cm^2/s from Eq. (7).

The initial steam density is taken as 0 $g \cdot cm^{-3}$. The steam density at mat surfaces as the boundary condition is of 0.001081, 0.002101, and 0.003132 $g \cdot cm^{-3}$ corresponding to steam pressure of 2, 4, and 6 kgf/cm^2, respectively. The steam evaporation condition at mat sides is given in Eq. (12) where the surface evaporation coefficient based on the steam density gradient, ρ has a value of 1.434 $cm \cdot s^{-1}$ [26].

The time increment for the calculation was 0.25 s. The factors and the levels of the numerical analysis on steam-injection pressing are summarized in Table 1.3. Two cases were analyzed to investigate the effect of the vertical density gradient of the mat on the temperature behavior of mat. One was given from the observed values for boards with average densities of 0.6 and 0.8 g/cm^3 and the other was for uniform density boards with densities of 0.3 and 0.4 g/cm^3.

Table 1.3 The factors and levels of the numerical analysis in steam-injection.

Mat moisture content (%)	Mat density (g/cm^3)	Mat thickness (mm)	Equilibrium vapor pressure in injection (kg/cm^2)	Steam-injection time (sec)
0	0.3*, 0.4*, 0.6**, 0.8**	10, 20, 40, 60, 100	2, 4, 6	1, 3, 10, 30, 60

* Flat vertical density profile.
** Vertical density profile based on the data.

1.2.3 Numerical procedure

The program for analysis of the two dimensional problem on heat transfer[22] was improved so as to allow analysis of the temperature distribution commonly in both hotpressing and steam-injection pressing. Figure 1.11 shows the flow chart of the FORTRAN program. The procedure is explained as follows:

1) First gridpoint co-ordinates and element numbers are input.

2) Before steam injection, the initial condition, the boundary conditions of the regulated mat surface temperature, and that of the heat outflow at the mat sides are input for the heat

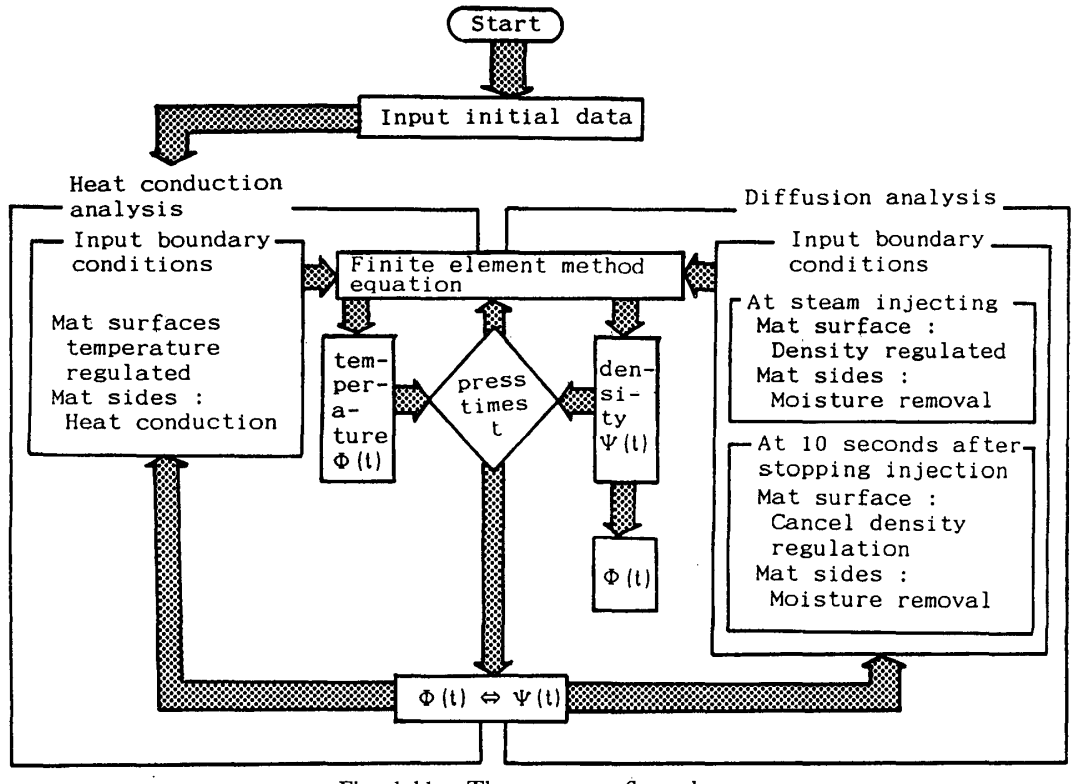

Fig. 1.11. The program flow chart.

conduction analysis. The temperature $\Psi(t)$ is calculated from the finite element equation, which is continued to be solved until the time step immediately before the diffusion analysis. In the analysis with hotpressing, the heat conduction analysis is continued to the end of the pressing time, while in that with steam injection pressing all grid point values are initiated at this time step.

3) During steam-injection, the boundary condition of the regulated steam density at the mat surface and that of the steam evaporation from mat sides are input. The steam density $\Psi(t)$ is calculated from the finite element equation obtained by these data. The equation which was substituted by the obtained $\Psi(t)$ at the next time step is continued to be solved. The initial value is taken before $\Psi(t)$ reaches the saturated steam density corresponding to the initial temperature. In output $\Psi(t)$ is converted into $\Phi(t)$.

4) Immediately after stopping steam-injection, the boundary condition of regulated steam density at the mat surfaces is cancelled.

5) After a further 10 s at the time stopping steam injection, $\Psi(t)$ which was obtained at the step 10 s after steam-injection is converted into $\Phi(t)$ and is put in as the initial values of the heat conduction equation. After the boundary condition of the regulated temperature and that of the heat outflow from the mat sides are input the heat conduction analysis is continued to the end of the pressing time.

1.2.4 Results and discussion

Figure 1.12 shows a comparison of the experimental results with a calculated temperature distribution along the mat thickness in steam injection pressing. The calculated temperature distribution in the inner layers agrees relatively well with the observed values during steam injection. The experimental values at mat surfaces, however, are slightly below 160°C. In the experiment, temperature increase was delayed by the Teflon sheet (0.1 mm thick) inserted between mat surface and hotplaten, and the thermocouples sank a little into the mat during pressing. After steam-injection the experimental values for a 20 mm thick mat decreased by about 10°C and then increased gradually again. It seems that the flux and influx of steam got out of balance after steam injection had been stopped, and that the condensed moisture in mat withdrew latent heat from the mat. The theoretical values of temperature increased after a slight decrease, because interaction between injected steam and particles is neglected in the program. Just after steam injection, the experimental temperature values increased slightly more than those of the theoretical values. This is probably due to the absorption heat generated in the wood particles.

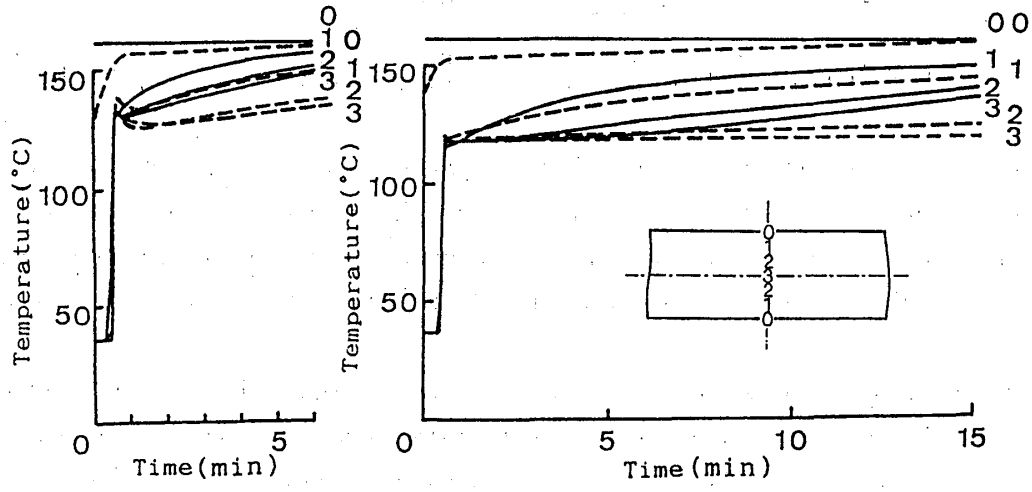

A) Mat density 0.4 g/cm^3, Mat thickness 20 mm.

B) Mat density 0.4 g/cm^3, Mat thickness 40 mm.

Fig. 1.12. Comparison of experimental and calculated results of the temperature distribution along the mat thickness in steam-injection pressing.
(Steam pressure 4 kgf/cm^2, Injection time 3 sec, Mat moisture content 0%, ———: calulated values, – – –: experimental values (The positions of the thermocouples are 0, 1, 2, 3 from the top graph in each case)).

Figure 1.13 shows the effect of steam pressure on the core temperature-time curves in steam-injection pressing. Core temperature immediately after steam injection rose with an increase of steam pressure for both 20- and 40-mm-thick mats.

Figure 1.14 shows the calculated results of the effect of mat density on the core temperature curves in steam-injection pressing. The increase of mat density does not significantly affect the

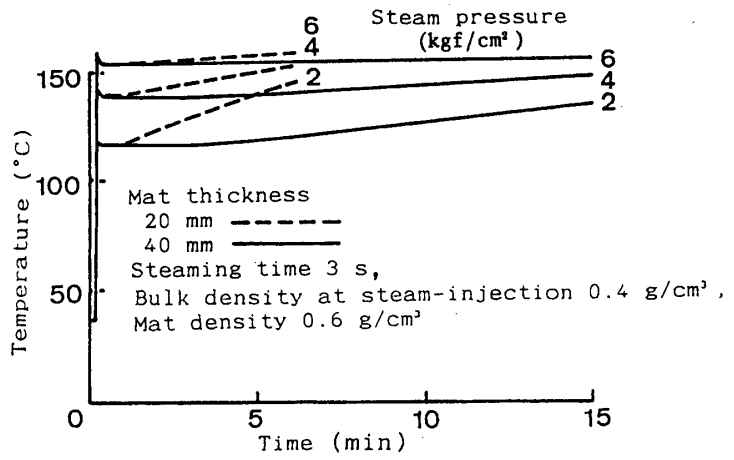

Fig. 1.13. Calculated results of the effect of steam pressure on the core temperature curves in steam-injection pressing.

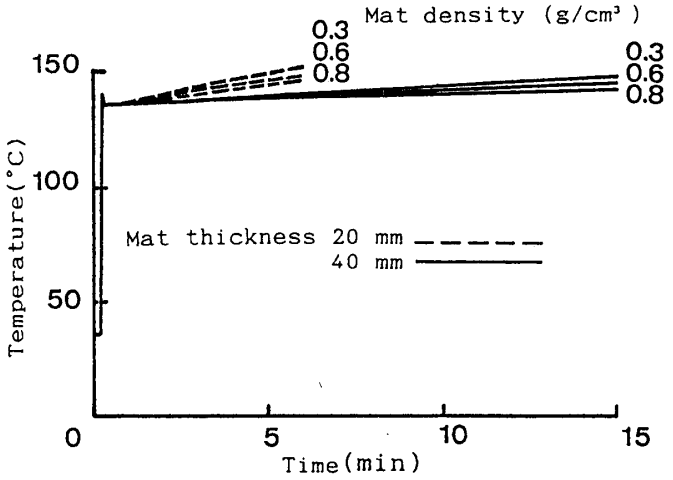

Fig. 1.14. Calculated results of the effect of mat density on the core temperature in steam presing.
Note: Steam pressure=4 kgf/cm^2, injection time=3 sec, bulk density at steam injection=0.4 g/cm^3 (0.3 g/cm^3 bulk density for 0.3 g/cm^3 mat).

mat core temperature by steam-injection. The rate of temperature increase after steam injection, however, decreases slightly with an increase in mat density because of the increase in thermal capacity of the whole mat.

Figure 1.15 shows the calculated results of the relationship between mat thickness and steam injection time necessary for a mat core to reach 100°C. With increase in mat thickness, the injection time required to reach 100°C increases. It is apparent that about 8-s-steam-injection is required for the core of 1000-cm-thick mat to reach 100°C, the temperature necessary for an isocyanate resin to cure within 1–2 min[17,27]. Therefore, the simulation predicts that such a thick board can be produced with a 2–3 min press time by steam-injection pressing.

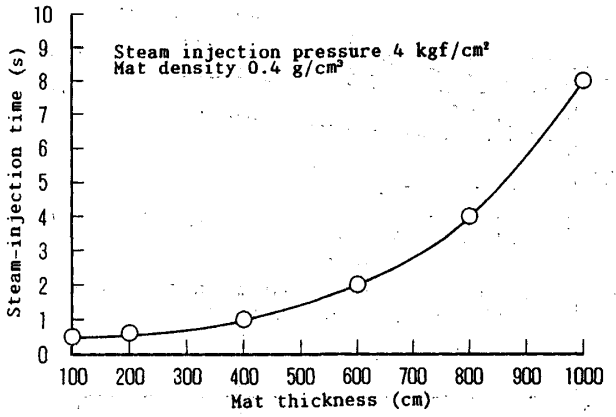

Fig. 1.15. Calculated results of the relationship between mat thickness and steam-injection time necessary for mat core to reach 100°C.

1.3 Summary

The temperature behavior of the particle mat during hot-pressing and steam-injection pressing was investigated under various conditions. With an increase of moisture content, the time necessary for the middle layer to reach 100°C tended to shorten, whereas the time to maintain a constant temperature (about 100°C) was prolonged in the case of hotpressing. The temperature in the middle layer of a mat with a higher moisture content in the face layers increased more than that of a mat with a uniform distribution of moisture content. In the case of steam-injection pressing, the temperature in the middle layer of the mats immediately increased to a specific degree decided by injection pressure and the characteristics of mats at the moment of steam-injection, and maintained a constant level during steam-injection. After stopping steam-injection, the temperature decreased a little, and then started to rise again. The rates of temperature increase in the middle layers of mats were independent of thickness, moisture content and density in the range of the experimental conditions.

The temperature distribution in particle mats during steam-injection pressing was numerically analyzed with the finite element method under various conditions. Calculated results agreed comparatively well with the observed results, which proved that the analytical theory was useful to predict the temperature behavior of particle mats during steam-injection pressing. In steam-injection pressing, with increases of mat thickness, the injection time necessary for raising core temperature up to 100°C gradually increased. For example, it will take about 8 s for the core temperature of a 1000-cm-thick mat, to reach 100°C.

Chapter 2 Steam Diffusion in Particle Mat During Steam-injection Pressing

In the process of steam-injection pressing, it is very important to know the influence of the particle geometry on the steam diffusion because steam is the main medium to control the heat energy through the particle mat. The curing conditions of adhesives depend very much on how the steam diffuses in the mat. The compaction ratio (CR: board

density/particle density) of particles and pressing conditions are considered as important factors that influence the diffusion of steam in the mat[28].

In the previous chapter, the mechanism of heat flow in the mat with steam-injection pressing was discussed and the optimum production conditions were determined. This chapter discusses the effects of particle geometry, CR, and pressing conditions of the steam-injection on the temperature behavior in the mat and the air permeability of the boards.

2.1 Effects of particle geometry on temperature behaviors in particle mats[24]

2.1.1 Experimental

Regulation of particles

A series of model particles of regulated sizes in three dimensions were prepared as follows: First, the boards with a thickness corresponding to the required particle width were cut from sawn lumber of Japanese red pine (*Pinus densiflora* Sieb. et Zucc.) with an air-dry density of 0.4 g/cm^3. Second, the boards with a width equal to a needed particle length were cut into blocks across the grain. Third, the blocks after having been soaked in water for a day were cut to a certain thickness with a cross section disk planer.

Seven kinds of particle sizes, that is, the particle lengths (l) of 10, 20, 50, and 80 mm, widths (w) of 2 and 10 mm, and thicknesses (t) of 0.3, 0.6, and 0.9 mm, were prepared. The standard particle length, width, and thickness is 20, 2, and 0.3 mm, respectively. Dimensions of each particle were measured to calculate the mean and the standard deviation which are shown in Table 2.1. As the particles were prepared with strict control of particle

Table 2.1. Model particle configuration.

a. Prepared particles.

Particle No.	l (mm)	w (mm)	t (mm)	Particle No.	l (mm)	w (mm)	t (mm)
1	10	2	0.3	5	20	10	0.3
2	20	2	0.3	6	20	2	0.6
3	50	2	0.3	7	20	2	0.9
4	80	2	0.3				

b. Measurement of particle size.

l (mm) Target	l (mm) Measured	S.D.	C.V. (%)	w (mm) Target	w (mm) Measured	S.D.	C.V. (%)	t (mm) Target	t (mm) Measured	S.D.	C.V. (%)
10	10.02	0.04	0.00	2	2.04	0.05	0.02	0.3	0.303	0.03	0.10
20	20.01	0.02	0.00	10	9.99	0.10	0.01	0.6	0.602	0.02	0.04
50	49.99	0.06	0.00					0.9	0.906	0.04	0.04
80	79.92	0.27	0.00								

Legend: l, w and t: Particle length,width, and thickness, respectively. S.D. and C.V.: Standard deviation and coefficient of varience, respectively.
Note: The number of particles measured in each configuration=50–100 particles.

sizes, the variations of coefficients were very small.

Temperature behaviors in mats

No binders were applied to the particles with the moisture content of 0% for convenience. The temperature distribution in the middle layer was measured by means of copper-constantan thermocouples with wire diameters of 0.2 mm connected to a porous glass-fiber reinforced teflon sheet that was inserted into the center layer. These were connected to a data processor via a data logger, and the temperature at each point was recorded at time intervals. Fig. 2.1 shows the locations of each measuring point in the mat plane. The temperature at nineteen spots were measured. The error was estimated to be ±0.5°C.

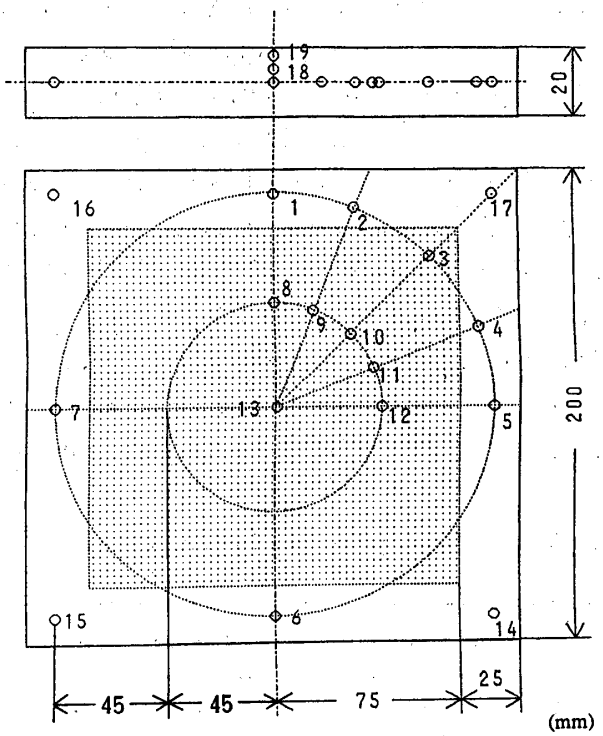

Fig. 2.1. Location of thermocouples in mat.
Note: The mesh shows an area of steam perforations.

For the steam-injection pressing, a set of 550×550×30 mm perforated plates were prepared to fit the surfaces of the hot-platens of the conventional hot-press. The upper and lower plates were perforated with a hundred and forty-four 2 mm-diameter holes drilled through half the depth of the plates with a 25×25 mm spacing pattern, which covered an area of 150×150 mm of each plate.

The temperature measurements started at the moment when pressure was applied to a particle mat. Steam was injected into the mat at a mat density of 0.2 and 0.4 g/cm^3 for the target density of 0.4 g/cm^3, and 0.2 and 0.6 g/cm^3 for the target density of 0.6 g/cm^3, for three seconds. The temperatures were recorded every two seconds. The initial steam pressure were 2, 4, and 6

kgf/cm^2 ; upper and lower hot-platens were regulated at the same temperature of 160°C, the mat size was 20 (t)×200×200 mm, and the total pressing time was 3.5 min.

2.1.2 Results and Discussion

A uniform temperature distribution in the middle layer of the mat was observed in the steam-injection. As the mat plane was symmetric in two directions, the average of twelve spots in one-forth part of the whole plane is discussed in this paper. The temperature of two spots between the center and the surface always started increasing earlier than the others. This behavior gave us a clue for deciding the start of steam-injection.

Fig. 2.2 shows the effects of particle lengths on the temperature behaviors in the middle layers. The rate of temperature increase after steam-injection becomes less at the length of 50 mm than for other lengths in the case of 2 mm wide particles. A remarkable difference was observed by changing the particle length in the case of 10 mm wide particles. The temperature increased more slowly with increases of particle lengths. It took more than 3 min to reach the temperature of 100°C, that is, the temperature for isocyanate resin to cure in a minute. The resistance for steam to diffuse in the mat became greater with longer particles. The temperature

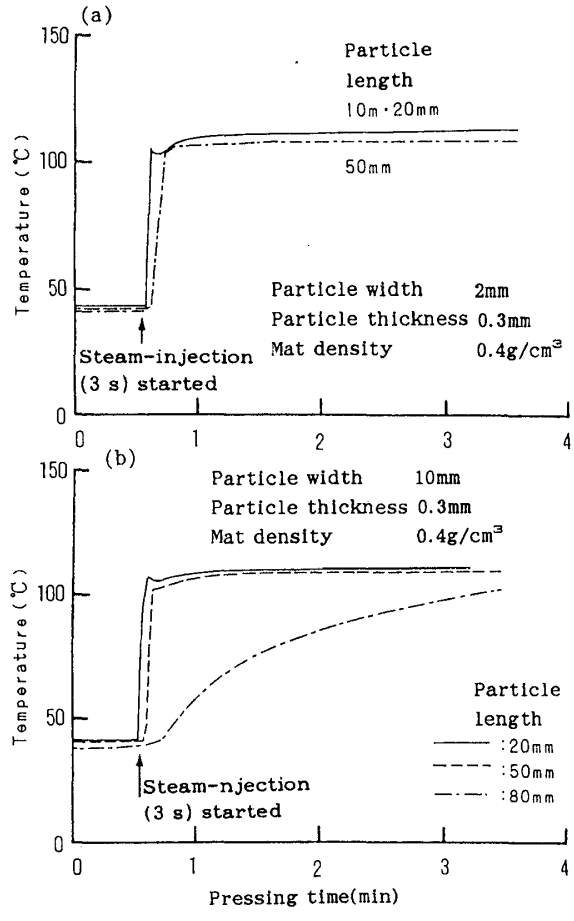

Fig. 2.2. Effect of particle length on temperature behavior of mat core.

behavior in the case of 80 mm long particles was the same as that in the mat of which the moisture content before pressing was 11%[17]. This means that the steam did not reach the middle layer, and that the temperature increased by heat conduction.

Fig. 2.3 shows the effect of the particle thickness on the temperature behavior in the mat. The rate of the temperature increase is greater as the particle thickness increases after increasing more than 100°C by steam-injection. The number of voids seen on the sides of the manufactured boards increased by increasing particle thicknesses, when the other two dimensions were constant. It seems that these voids have an influence on the rates of temperature increases.

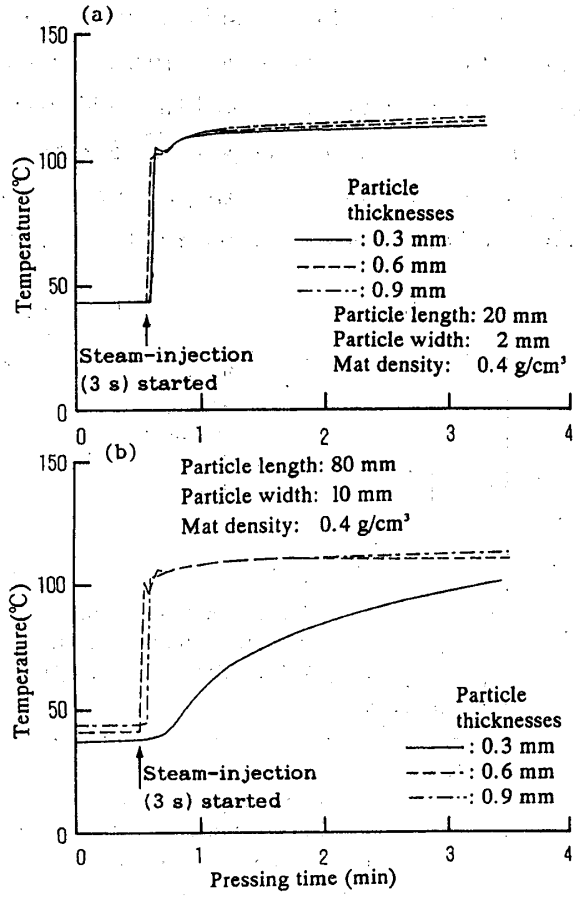

Fig. 2.3. Effect of particle thicknesses on temperature behaviors of mat cores.

Fig. 2.4 shows the effects of mat densities at injection on the temperature behaviors in the middle layers. In the case of 0.4 g/cm^3 density board, the temperature started increasing at the moment that steam was injected, whereas in 0.6 g/cm^3 density board, the start of temperature increase was delayed. In the latter, there was a time lag in the case of the 0.2 g/cm^3 mat density at injection. This may have been due to the fact that it is more difficult for steam to flow in a mat with a greater thickness in spite of the same mat density. It took about 15 s before the

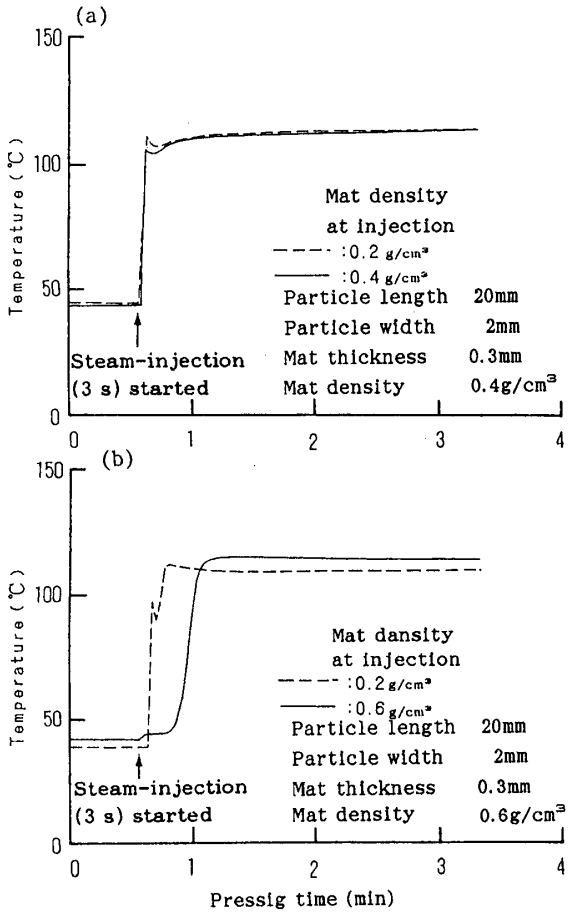

Fig. 2.4. Effect of mat density at temperature behaviors of mat core.

temperature in the middle layer started increasing when steam was injected at the mat density of 0.6 g/cm^3. The maximum temperature achieved by steam-injection was greater in the case of 0.6 g/cm^3 density board because of greater steam pressure in the mat.

The effect of the initial steam pressure also was examined. However, no apparent differences of temperature behaviors were seen in the range of 2 to 6 kgf/cm^2 initial steam pressure.

2.2 Effects of particle geometry on the gas permeabilities of boards[24)]

2.2.1 Experimental

Measurements of air permeabilities of boards

Under the same conditions as those of the temperature behavior experiment, two boards with dimensions of 10×340×340 mm were produced for each level of particle geometry and pressing condition. That is, the mat density at injection was 0.2 and 0.4 g/cm^3 for the target density of 0.4 g/cm^3, and 0.2 and 0.6 g/cm^3 for that of 0.6 g/cm^3, the steam-injection time was three seconds, and the initial steam pressure were 2, 4, and 6 kgf/cm^2.

Adhesive used was an isocyanate compound resin, UL-4811 formulated by Gunei Kagaku

Kogyo Co. Ltd. Acetone was added at 20% based on resin solids to reduce the viscosity of the adhesive. The resin was sprayed on the particles (having a moisture content of 12%) using a drum-type rotary blender by means of an airless gun. The resin content was 10% of the resin solids/dried particle weight. Hand-formed particle mats were pressed in a hotpress with the temperature of 160°C. Both top and bottom surfaces of the particle mats were covered with porous glass-fiber reinforced Teflon sheets so as to prevent the mat from sticking to the platens. The total pressing time was 1.5 min.

The sample boards were conditioned for two weeks at 20°C and 65% RH, followed by the cutting of test specimens for use in measuring the air permeability.

Fig. 2.5 shows the system[29] for measuring air permeability. The specimens were rectangular blocks, 100×10×10 mm, for measuring the air permeability in the direction horizontal to the heat platens and three to five piled cubes with each having a size of 10×10×10 mm for measuring in a vertical direction. Before starting the measurements, the sides of each specimen were covered with plastic film. Then, each specimen was inserted into a plastic tube to prevent the leakage of air. Air was flowed through the specimens from the end by a micro-feeder at the flow rate of 4.80×10^{-3} to 1.78×10^{-2} cm^{-2}/s, and the pressure was measured at a steady state. The permeability was estimated by the following equation of Darcy's law:

$$k_p=(Q\cdot P\cdot L)/(\Delta P\cdot A\cdot \bar{P}) \quad (19)$$

where, k_p: air permeability, cm^3 (air)/cm·atm·s,

Q: volumetric flow rate, cm/s,

P: air pressure, atm,

L: length of the specimen in the flow direction, cm,

ΔP: air pressure difference between the specimen edges, atm,

A: cross-sectional area of the specimen, cm,

$\bar{P}$: average air pressure of the specimen, atm.

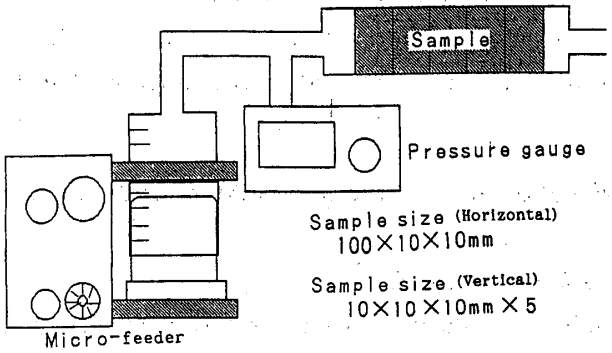

Fig. 2.5. System for measuring air permeability.

2.2.2 Results and discussion

Air permeabilities of boards

Fig. 2.6 shows the effects of particle lengths on the air permeability. The air permeability

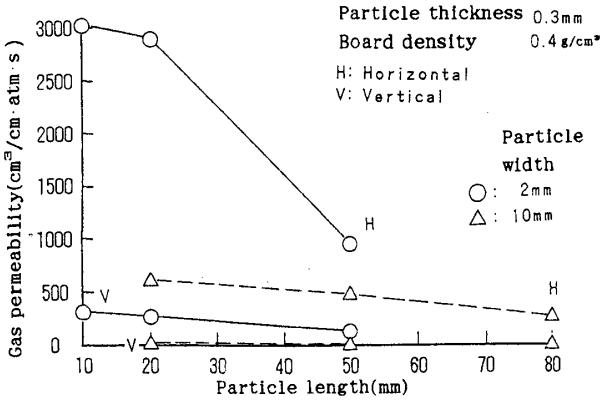

Fig. 2.6. Effect of particle length on gas permeability of boards.

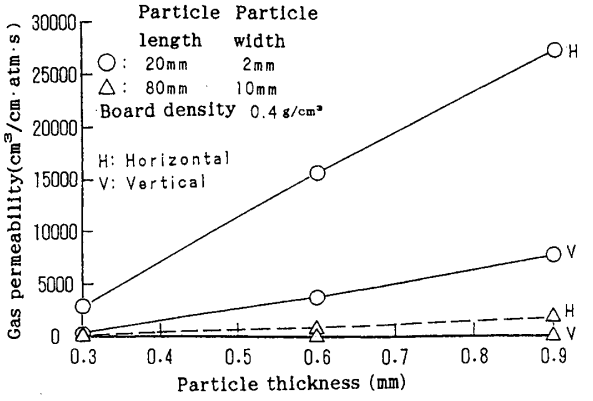

Fig. 2.7. Effect of particle thicknesses on gas permeability of boards.

decreased with increases of the particle lengths when the particle thicknesses and widths were constant. It decreased as well with increases of the widths at the same length. The air permeability in the horizontal direction was always greater than in the vertical direction. Fig. 2.7 shows the effects of the particle thicknesses on the air permeabilities. The air permeabilities of both horizontal and vertical directions tended to increase with increases of the particle thicknesses.

These results of the air permeabilities of boards well explains those of the experiment on temperature behaviors through the particle mats during steam pressing.

Fig. 2.8 shows the effect of the mat densities at injection on the air permeabilities of manufactured boards. The air permeabilities of boards were independent of the mat densities at injection. This may have been due to the fact that permanent paths are not formed by steam injection and that the injected steam diffuses through the paths between the particles which already existed because if any paths had been formed by the steam-injection, there should have been influences on the air permeability of the boards produced by changing the injection timing.

Fig. 2.9 shows the effects of board densities on air permeabilities. The greater the board density, the less the air permeability. The air permeability was remarkably greater at the CR of

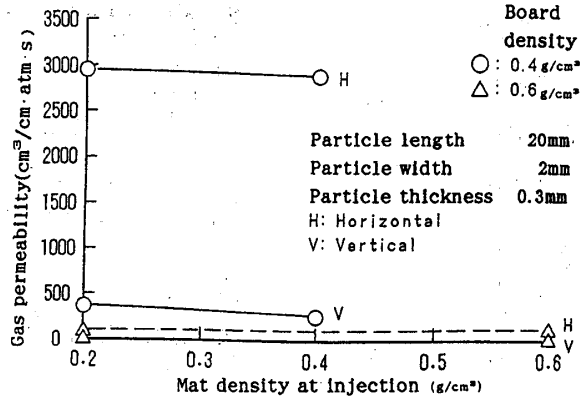

Fig. 2.8. Effect of mat density at injection on gas permeability of boards.

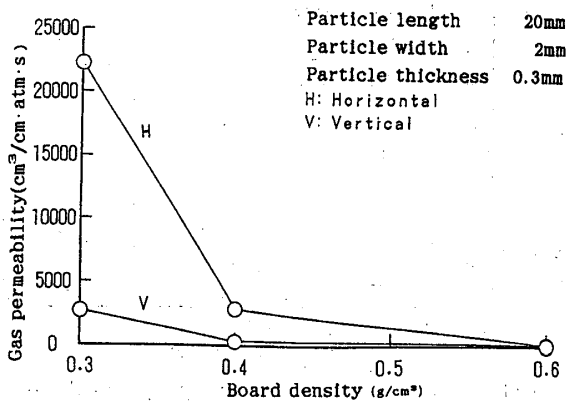

Fig. 2.9. Effect of board density on gas permability of boards.

0.75. This may have been due to the fact that the resistances against the steam flows in the mats become less because the voids among particles increased with decreases of CRs. As the range of the vertical line is greater in the figure, the air permeability for the horizontal direction appears to be equal to that for the vertical direction at a 0.6 g/cm^3 board density; however, in fact, the former was about 25 times as great as the latter. Boards with a greater CR always have lower air was about 25 times as great as the latter. Boards with a greater CR always have lower air permeabilities. The ratios of air permeabilities in horizontal and in vertical directions are 3–400, depending on the particle sizes and CRs.

Fig. 2.10 shows the effects of the initial steam pressures on the air permeabilities of boards. With increases of the steam pressures, the air permeabilities of boards in a horizontal direction decrease, whereas that in a vertical one increase. Thus the difference of the permeabilities in the two directions decrease. This may be due to the fact that wood particles deform non-elastically by the injected steam, and the contact area of each particle becomes greater. This result suggests the possibility of developing products with more uniform and with greater dimensional stabilities by injecting steam with greater pressures.

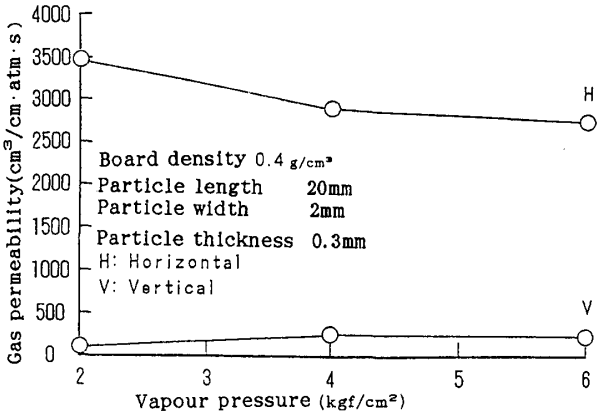

Fig. 2.10. Effect of steam-injection pressure on gas permeability of boards.

Multiple regression analysis[30)]

The influences of the particle geometry and the timing of the injection on air permeability were analyzed by multiple regression analysis. The program used was "micro-CDA" developed by Professor T. Haga. In this program, degrees of freedom double adjusted coefficients of determination are used for the standard of the selection of variables, and a stepwise regression procedure also is used. The obtained equation by this analysis is as follows:

$$k_{ph}=1{,}110l-4{,}540w+531{,}450t+700w\cdot l$$
$$-63{,}300t+1.1\exp(15.42-7.32CR)-14{,}252 \quad (20)$$

$$k_{pv}=590l-260w+163{,}460t$$
$$-20{,}300l\cdot t+1.14\exp(13.87-8.12CR)-4{,}915 \quad (21)$$

where k_{ph}: gas permeability in the horizontal direction [cm^3 (air)$\cdot cm^{-1}\cdot atm^{-1}\cdot s^{-1}$], k_{pv}: gas permeability in the vertical direction [cm^3 (air)$\cdot cm^{-1}\cdot atm^{-1}\cdot s^{-1}$], l: particle length [cm], w: particle width [cm], t: particle thickness [cm], and CR: compaction ratio.

When a linear regression equation with only variables of length, width, and thickness of particles, the degrees of freedom double adjusted coefficients of determination are less for both directions. By adding the predictor variables of $w\cdot l$, $l\cdot t$ and CR to Eq. (20), and $l\cdot t$ and CR to Eq. (21), each of the degrees of freedom double adjusted coefficients of determination show the large values of 99.6% and 99.7%, respectively. Thus, the diffusion phenomena of air in mats can be interpreted as follows: air, not only move linearly, but also diffuse in two dimensions through between the particle surfaces. It may be concluded that the steam diffusion in the whole mat is the phenomena that is resulted from the repetition of the diffusion among particle surfaces in two dimensions.

Eqs. (20) and (21) are valid only under the conditions of this experiment. However, it is important to predict the air permeabilities of boards in extreme conditions in developing new materials. When both the equations are valid out of the range of this experiment and each material is very small, such as powder, then

$k_{ph}<0$ (l, w, $t\to 0$),

$k_{pv} < (l,\ w,\ t \to 0)$.

On the other hand, when t is a constant, and l and w are greater such as in sawn boards, it is obvious from the signs of Eqs. (20) and (21) that the next relationships should be held:

$k_{ph} < 0$,

$k_{pv} < 0$.

Therefore, it is predicted that the air permeabilities approach 0 in either case of much smaller or greater particle sizes.

2.3 Summary

Each of seven types of Japanese red pine particles with different dimensions, strictly controlled for length, width, and thickness, was prepared in order to investigate the temperature behavior in the mat, and the air permeability of the boards with specific gravities of 0.30–0.60. The variables influencing the temperature behavior in the mat by steam-injection press is directly related to the air permeability of mats. The air permeability of the boards in the horizontal direction to the heat platen is always higher than in the vertical direction. A functional equation with a higher coefficient of determination that explains the air permeability is obtained by a multiple regression analysis. It is inferred that the temperature increase in the mat result from the repetition of the steam diffusion among particles in two dimensions.

Chapter 3 Physical and Mechanical Properties of Particleboard Produced by Steam-injection Pressing

In the production of boards with the steam-injection pressing, the production factors auch as injection time, injection timing, pressing time, and the way how steam diffuse in the mat are important because they decide the properties of final products.

In the previous chapter, the mechanism of heat flow in the mat was discussed and the effects of particle geometry, CR, and pressing conditions of the steam-injection on the temperature behaviors in the mat and the air permeabilities of the boards.

In this chapter, firstly the effect of injection timing and injection time on physical properties of boards are examined. Secondly, 20-mm-thick isocyanate bonded particleboards were manufactured with various total press time under the obtained conditions and then the effect of total press time on physical properties of boards were examined. Finally, the physical and mechanical properties of boards produced with various particle size and pressing conditions.

3.1 Effect of steam-injection time and timing on board properties[31]

3.1.1 Experimental

Raw materials used were Seraya (*Shoren* spp.) end-logs with an air dry density of 0.4 g/cm^3. Chips of the materials prepared by drum chipper were converted into flake-type particles with a knifering flaker (Pallmann PZ-8). The average dimensions of particles

were 9.1 mm long, 0.28 mm thick and 5.7 mm long, 0.38 mm thick for the experiment on steam-injection time and for that on injection timing, respectively. One half part of the particles were dried with a vacuum dryer to about 0% moisture content for steam-injection pressing, in order to investigate only the influence of injected steam and the remainder was conditioned to 11% moisture content for conventional pressing.

Resin binder used was an isocyanate compound (IC) adhesive, UL-4800, formulated by Gun-ei Kagaku Kogyo Co. Ltd. The resin content level was 10% of resin solid, based on oven-dry weight of particles. To obtain a suitable viscosity of adhesive for spraying, acetone was added to the IC resin at 20% based on the weight of resin solids. The resin was sprayed on the particles in a drum-type rotary blender by means of an airless gun. Hand-formed particle mats were pressed at 160°C. Both upper and lower surfaces of the mat were covered with teflon coated glass-fiber nets to prevent the mat from sticking to the platens. Target board densities in an air-dry condition were 0.4 and 0.6 g/cm^3, and the dimensions of the boards were 500×450×20 mm.

In the experiment on the effect of steam-injection time, the target steam pressure was 6 kgf/cm^2 (160°C) with an effective steam pressure of 4 kgf/cm^2 (140°C). Steam-injection time was varied at 3, 10, and 30 s. Steam was injected 30 s after the start of press pressure build-up. The total pressing-times were 3.5 and 5.5 min for steam injected- and conventional pressed-board (no steam-injection), respectively.

In the experiment of steam-injection timing, steam was injected in the bulk densities of 0.3 and 0.4 g/cm^3 for board density of 0.4 g/cm^3, and 0.3, 0.4, 0.5, and 0.6 g/cm^3 for board density of 0.6 g/cm^3. Steam-injection time was 3 s with an effective steam pressure of 4 kgf/cm^2. Total press times were 3 min for all boards.

Specimens cut from the above boards were tested after conditioning for 2 weeks at 20°C and 65% relative humidity (RH). Modulus of elasticity (MOE) and modulus of rupture (MOR) both in air-dry and wet conditions, internal bond strength (IB), screw withdrawal resistance (SW) in air-dry condition and thickness swelling (TS) after a 24-h-water-immersion were measured according to Japanese Industrial Standard (JIS) A5908. For the wet treatment in the bending test the specimens were boiled for two hours and then immersed in water for one hour at a room temperature. Density distributions across thickness were determined by measuring weight and dimensions of specimens at each of sanding from the surface to core.

3.1.2 Results and discussion

Effect of steam-injection time

Density profiles across thickness of boards produced by conventional and steam-injection pressing are shown in Figure 3.1. From the Fig. 3.1, it can be understood that different density distributions across board thickness were produced by conventional and by steam-injection pressing; In conventional pressing, the density distribution across board

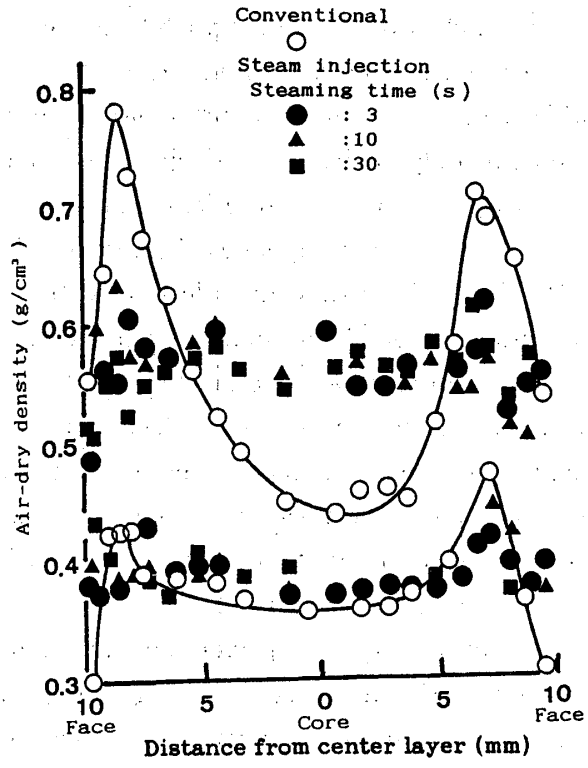

Fig. 3.1. Density profiles through the thickness on boards.

thickness showed a "U"-shaped distribution with higher density layers near the both surfaces and a low-density layer in the core. In steam-injection pressing, however, this distribution was rather uniform. In the case of steam-injection pressing, steam was used as a medium of heat transfer and it diffuses through the particle mat much faster than heat conduction. Consequently, temperature in all parts of particle mats suddenly increased in the very short time[17,21], and uniform plasticization through the particle mat occurred under high steam pressure. Wood particles remarkably plasticize under an unsteady state of both moisture and heat.

The effect of steam-injection time on density distribution across board thickness was not significant for 20 mm thick steam-injection pressed-board. This proves that 3-s-steam-injection gives the uniform plasticization of the whole particle mat.

In the case of conventional pressing, the difference of density between surface and core layers of particleboards with a density of 0.6 g/cm^3 is greater than that of 0.4 g/cm^3. This uniform density distribution of steam-injection pressed boards across thickness will give certain improvement of IB and dimensional stability, but a little decline in bending properties, as described in the following paragraph.

Figure 3.2 shows the effect of steam-injection time on MOE and MOR of boards under both dry and wet conditions. The MOE and the MOR of steam-injection pressed boards with a density of 0.6 g/cm^3 showed a little lower values than those of conventionally pressed boards.

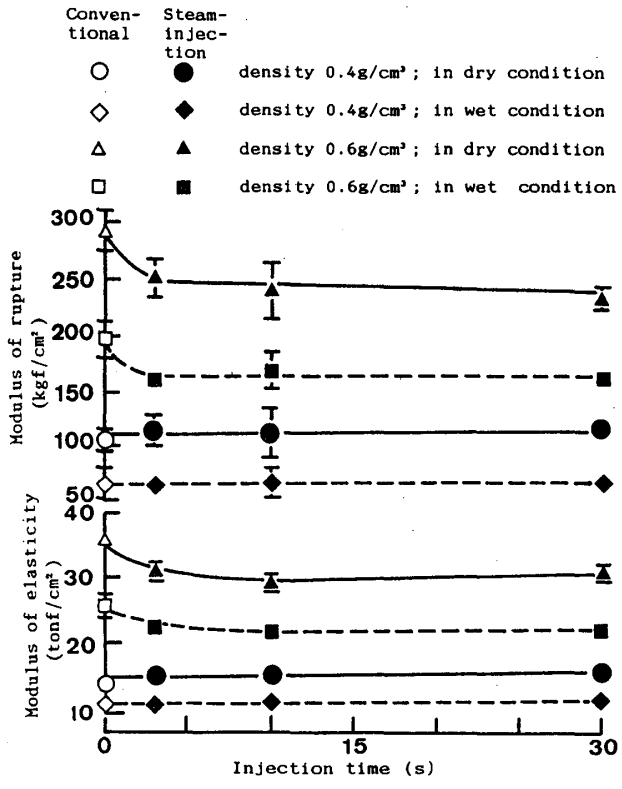

Fig. 3.2. Relationships between steam-injection time and modulus of elasticity and modulus of rupture in dry and wet condition. Legend : The ranges of the mean values show 95% confidence intervals.

This can be explained by the difference in density distribution across board thickness. Bending properties of particleboard depend mostly on stiffness and strength of surface layers. Boards produced by conventional pressing have dense surface layers, which was more favorable for bending properties than boards with homogeneous density profile produced by steam-injection pressing. The effects of steam-injection time on MOE and MOR were, however, not significant for both board densities of 0.4 and 0.6 g/cm^3. The bending strength of boards with a density of 0.4 g/cm^3 showed almost the same value as those of boards produced by conventional pressing in the same target density.

Furthermore, the figure suggests that a board with a thickness of 20 mm can be produced with very short steam-injection as 3 s ; namely, 3-s-steam-injection can raise the core temperature of particle mat to enough level for curing adhesive[17], as predicted in Fig. 2.18.

The relationship between steam-injection time and internal bond strength (IB) is shown in Fig. 3.3. The IB value of particleboards with a density 0.6 g/cm^3 produced by steam-injection pressing were about 20 kgf/cm^2, that is, 2 times greater than that of particleboards produced by conventional pressing. Furthermore, IB values for boards with a density of 0.4 g/cm^3 produced by steam-injection pressing showed also a little higher than that of boards produced by

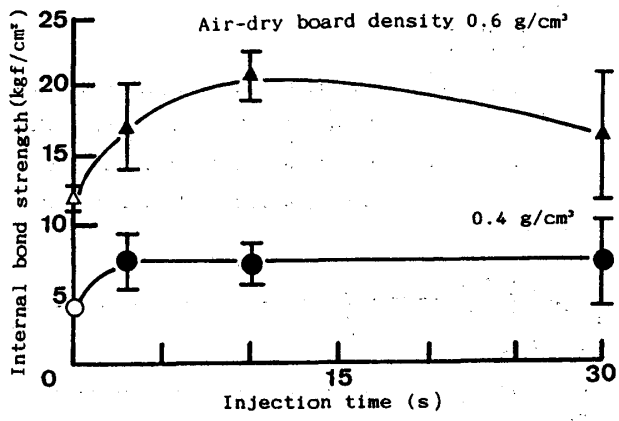

Fig. 3.3. Relationships between steam-injection time and internal bond strength.
Legend: ○, △: Conventional; ●, ▲: Steam injection. The ranges of the mean value show 95% confidence intervals.

conventional pressing. A linear correlation between IB and the density in the core layer (which is usually lower than in the surfaces in hot-platen pressed boards) has been found[13]. The results obtained in this experiment corresponded with the above mentioned report, since the density in the core of particleboard produced by steam-injection pressing is always higher than that of boards produced by conventional pressing.

In the range of this experiment, the screw withdrawal resistance (SW) of particleboards produced by steam-injection pressing did not depend on steam-injection time. The SW values of 31 and 72 kgf for board densities of 0.4 and 0.6 g/cm^3, respectively, were almost the same as those of boards produced by conventional pressing.

The relationship between steam-injection time and thickness swelling (TS) is shown in Figure 3.4. Similar TS values were observed in steam-injection pressed boards and hot-pressed

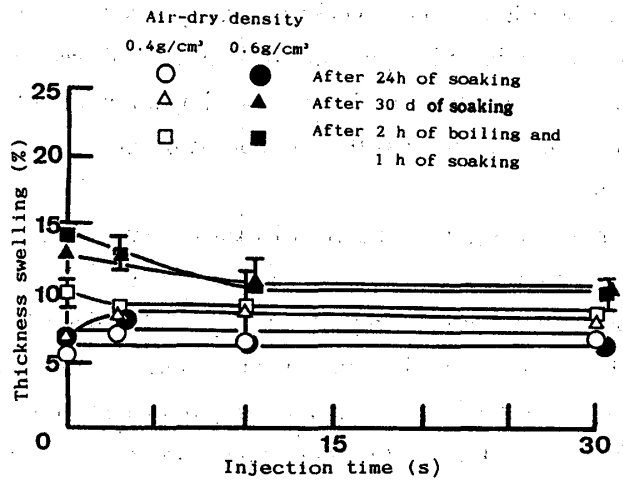

Fig. 3.4. Relationships between steam-injection time and thickness swelling.

boards for a density of 0.4 g/cm^3. On the other hand, the improvement of the dimensional stability was observed on steam-injection pressed boards with a density of 0.6 g/cm^3 when steam-injection time was more than 10 s. Thickness recovery of the dense surface layer formed during hot-pressing process seems to have greater influence on the TS[3,13,14]. In other words, the steam-injection pressed boards has the uniform density distribution across board thickness and results in better dimensional stability. High-pressure steam-treatment, also helps the relaxization of the internal stress which was built up in compressed particles during pressing[32]. As a result, steam-injection pressed particleboards have better dimensional stability than conventional boards, especially in high density range. Similar trend was observed in the accelerated aging test with 2-h-boiling or in 30-d-water-immersion.

Effect of steam-injection timing

The effect of steam-injection timing on MOE and MOR under wet and dry conditions is shown in Fig. 3.5. The effect of steam-injection timing on bending properties was not significant for board density of 0.4 g/cm^3 but was significant for board density of 0.6 g/cm^3. The MOE and the MOR values increased with delayed steam-injection timing. This corresponds with the tendency that delaying steam-injection timing forms surface layers with higher density.

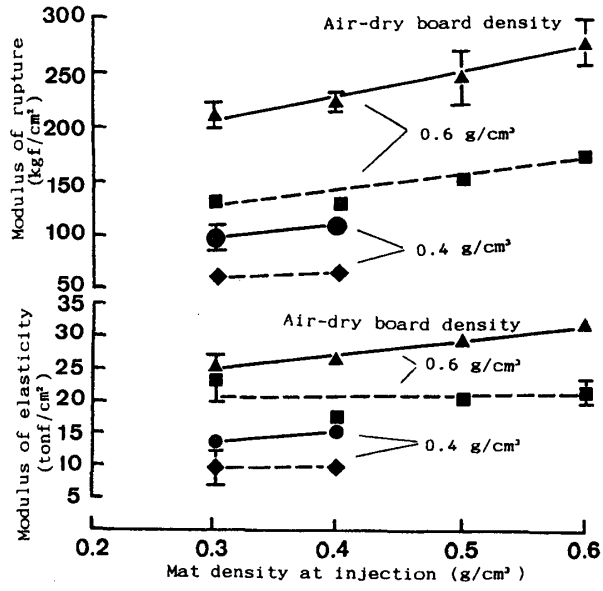

Fig. 3.5. Relationships between mat density at steam-injpture in dry and modulus of elasticity and modulus of rupture in dry and wet condition.
Legend : ●, ▲ : in dry condition ; ■, ◆ : in wet condition. The ranges of the mean value show 95% confidence intervals.

Figure 3.6 shows the relationship between steam-injection timing and IB. According to the above mentioned mechanisms of forming high density surface layer in conventional pressing, later steam-injection timing would form higher density surface layer and lower density core layer,

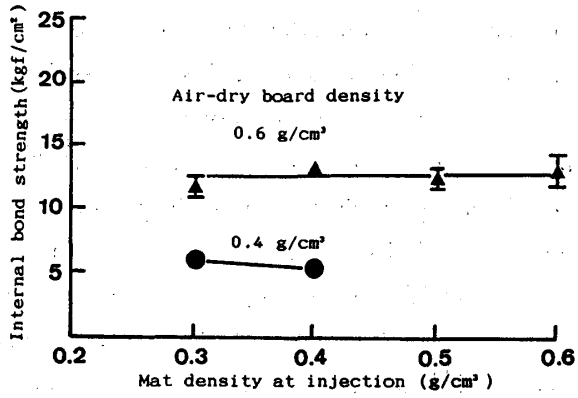

Fig. 3.6. Relationships between mat density at steam-injection and internal bond strength.

which results in a certain decrease of IB. However, the effect of steam-injection timing on IB was not clear on boards with 0.6 g/cm^3 density as shown in the Figure. This may be due to the negative effect of precure of adhesive which occurred when steam was injected at lower mat density. Namely, earlier injection timing compensates for the effect of higher core density.

The effect of steam-injection timing on TS is shown in Figure 3.7. Later steam-injection timing gave lower TS values for board density of 0.6 g/cm^3. From these experimental results, steam should injected when bulk density of mats increased up to a certain level where the particles had enough contact each other. In production of high density boards, greater compaction of particle mat is needed. Therefore, higher pressure and longer time are necessary to compress the mat to the target density. However, the press-time is shortened and less energy is required if steam is injected with an early timing. The economical choice of the injection timing results the injection at early stage in the press cycle. Considered the balance of these conflicts, the injection timing is better adjusted when the bulk density of mats reaches at least the compaction ratio of 1.0–1.3.

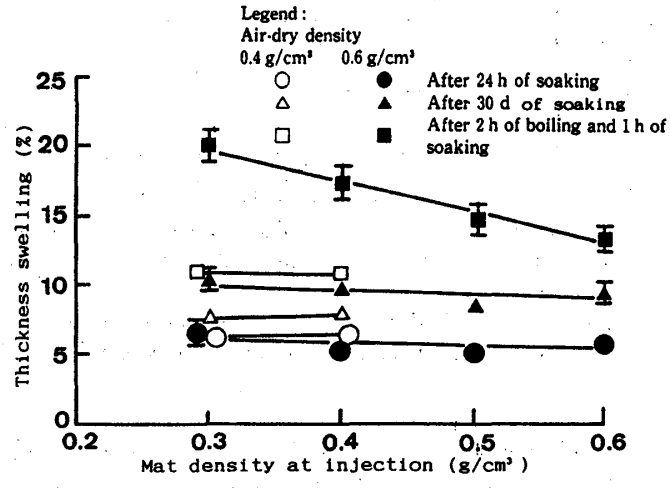

Fig. 3.7. Relationships between mat density at steam-injection and thickness swelling.

3.2 Effect of particle geometry on board properties[24)]

3.2.1 Experimental

Prepared materials and the methods of manufacturing the boards are the same as those of the experiment on the air permeability of boards in Chapter 2[24)]. Each of seven types of Japanese red pine particles with different dimensions, which are shown in Table 3.1, strictly controlled for length (l), width (w), and thickness (t), was prepared in producing particleboards with a density range of 0.3–0.6 g/cm^3 using an isocyanate compound adhesive under different pressing conditions.

Two experimental boards with a size of 10×340×340 mm were conditioned for two weeks at 20°C and 65% RH (relative humidity), followed by cutting test specimens for each level of particle geometry and pressing conditions. The mechanical and the physical properties of the boards were tested in accordance with Japanese Industrial Standard (JIS) A 5908. These were the modulus of elasticity (MOE), modulus of rupture (MOR), internal bond strength (IB), and thickness swelling (TS) after a 24-h-water-soak at 25°C. Statistical analyses of the data were made to determine the effects of the various factors on the board properties.

3.2.2 Results and discussion

Features of the voids among the particles from side views of the manufactured boards were as follows : as the particles became longer, more contact between them was observed, and the thicker the particles, the greater were the voids for both 2 and 10 mm wide particles. The sizes and distributions of the voids depended very much on the board densities. However, the injection timing and the initial steam pressure had little influences on the sizes and distributions of the voids.

Fig. 3.8 shows the effects of l, w, and t on MOR, and Fig. 3.9 shows their effects on MOE.

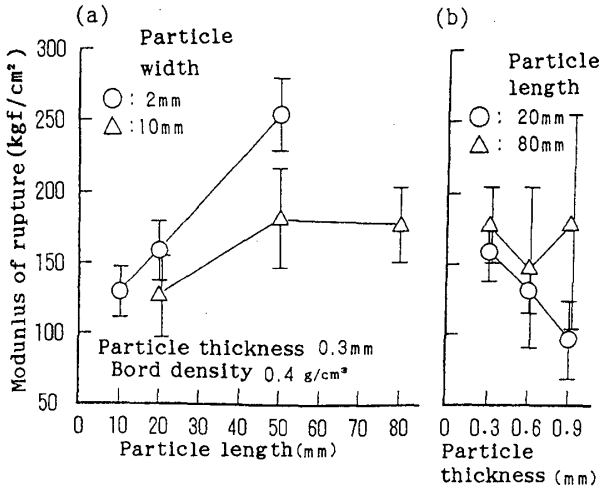

Fig. 3.8. Effect of particle configuration on the modulus of rapture.
Note: The ranges of the mean value show 95% confidence intervals.

The 0.4 g/cm^3 air-dry density boards surpassed the Type 200 of JIS in MOR in the case of 50 mm long, 2 mm wide, and 0.3 mm thick particles. The bending properties tended to increase with increases of l and with decreases of t (the latter at the length of 20 mm) when the other two dimensions were constant. This corresponded to the results for conventional boards. However, t had little influence on the bending properties at the length of 80 mm, and the bending properties had wide confidence intervals. This may have been due to the inhomogeniety of the steam diffusion in the mat. More steam diffuses between the sides of particles than between upper and lower particle surfaces when the particles are longer. Little difference in MOE compared to MOR, was shown at the same particle width resulting from less sensitivity in MOE for board structures.

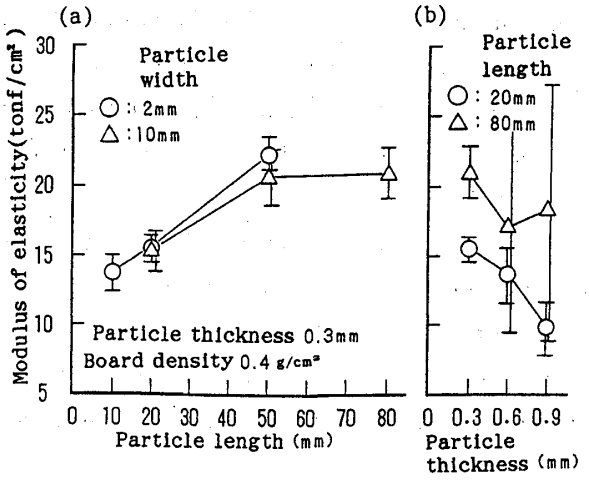

Fig. 3.9. Effect of particle configuration on the modulus of elasticity. Note: The ranges of the mean value show 95% confidence intervals.

Fig. 3.10 shows the effect of the particle geometry on the IB. Although the target board density is as small as 0.4 g/cm^3, greater IB value of about 6 kgf/cm^2 is obtained at 2 mm particle width, while it is lower value of about 1 kgf/cm^2 at 10 mm width. This may attribute to the lesser air permeability in the case of greater w. In general, the greater the thickness, the greater is the pressure applied on upper and lower particle surfaces. IB increased remarkably with increases of t in the case of 80 mm long and 10 mm wide particles. This corresponded to the results of previous studies[24]. With increases of t, larger voids could be seen in the cross-sections, and the air permeabilities showed their maximums at 0.9 mm particle thicknesses. However, IB decreased at 0.9 mm thicknesses in the case of 20 mm long and 2 mm wide particles. These decreases may have been due to the greater ratio of steam flowing between particle sides instead of moving between the upper and lower particle surfaces.

Fig. 3.11 shows the effect of the particle geometry on TS. TS increases with an increase of l. Although TS has the same tendency in the case of 10 mm long particles as that of previous studies,

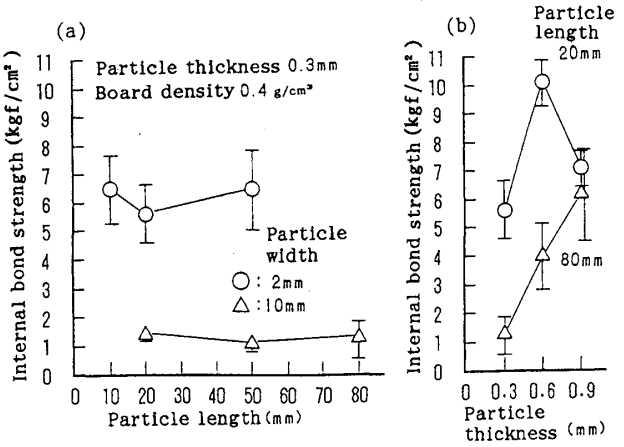

Fig. 3.10. Effect of particle configuration on the internal bond strength. Note: The ranges of the mean value show 95% confidence intervals.

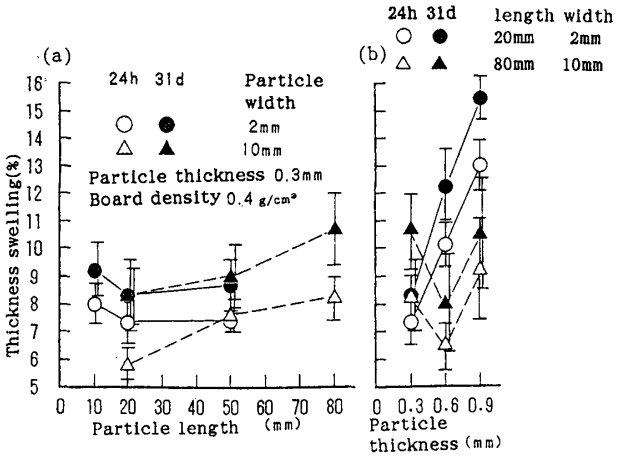

Fig. 3.11. Effect of particle configuration on the thickness swelling. Note: The ranges of the mean value show 95% confidence intervals.

it is almost independent of l in the case of 2 mm particle width. This may have been due to the inhomogeniety of the steam diffusion as mentioned before.

TS increased with an increase of t in the case of the 20 mm length and 2 mm width particles, whereas the TS decreased at the thickness of 0.6 mm, and little difference was observed between the TS at 0.3 mm and that of a 0.9 mm particle thickness. This may have been due to the lesser bonding strength at the 0.3 mm particle thickness resulting from the lesser air permeability in the mat.

Fig. 3.12 shows the effects of the mat densities at steam-injection on MOR and MOE. The larger MOR value of 350 kgf/cm^2 was obtained for 0.6 g/cm^3 density board. MOE and MOR were a little less at the mat density of 0.4 g/cm^3 at injection in the case of 0.4 g/cm^3 density board,

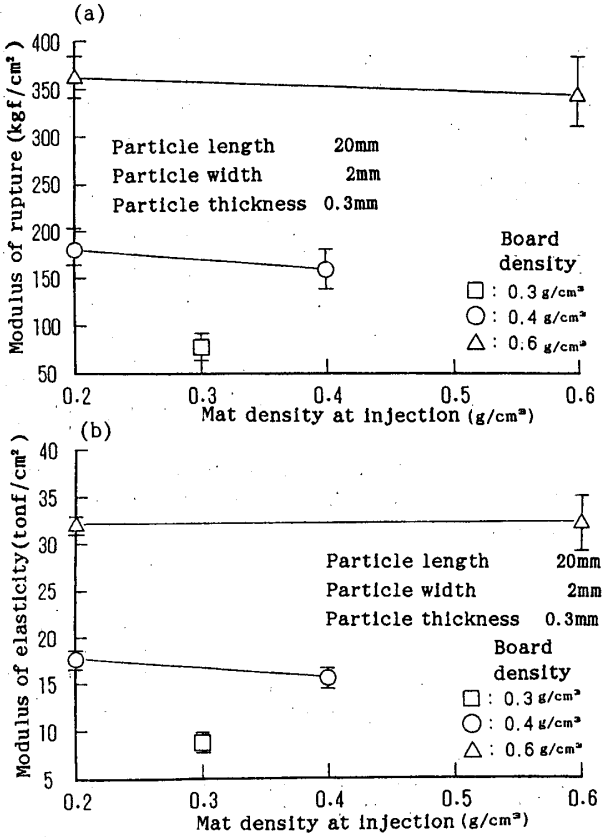

Fig. 3.12. Effect of mat density at injection on MOR and MOE.
Note: The ranges of the mean value show 95% confidence intervals.

whereas those of 0.6 g/cm^3 density boards seemed to be independent of injection timings.

Fig. 3.13 shows the effects of the mat densities at steam-injection on IBs and on TSs. IB was independent of the mat density at injection, whereas it was less at the mat density at injection for 0.6 g/cm^3 density board. This result can be predicted from the results of the temperature behavior in the mat. When steam is injected at a greater mat density, the temperature increases more slowly because of less air permeability in the case of the 0.6 g/cm^3 density board. On the other hand, little difference in temperature behavior was observed for 0.4 g/cm^3 density board, because the air permeability of the mat was large enough for the steam to diffuse in the mat at the smaller density of 0.4 g/cm^3.

The same tendencies were observed in the results of TS. The TS of 0.6 g/cm^3 density board after a 24-h-water-immersion was greater at the mat density at injection of 0.6 g/cm^3 because of lesser bonding strength between particles resulting from the smaller air permeability of the mat.

The effects of the initial steam pressure on board properties also were investigated. However, little differences were observed with an initial steam pressure range of 2 to 6 kgf/cm^2.

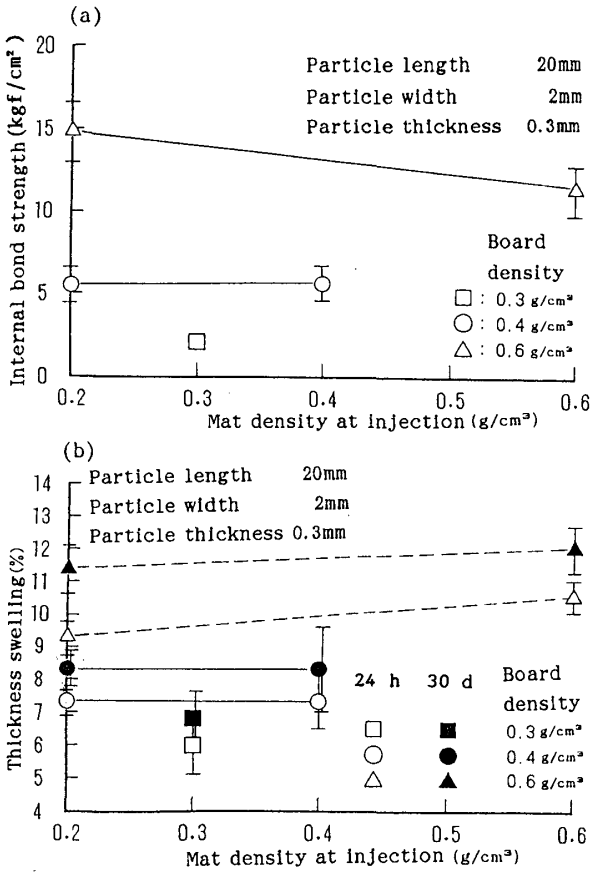

Fig. 3.13. Effect of mat density at injection on the internal bond strength and on the thickness swelling.
Note: The ranges of the mean value show 95% confidence intervals.

3.3 Shortening press cycle with steam-injection pressing[33)]

3.3.1 Experimental

Raw material used was Seraya (*Shorea* spp.) with an air-dry density of 0.4 g/cm^3. Chips of the materials prepared by a drum chipper were converted into flake-type particles with a knifering flaker (Pallmann PZ-8). The average dimensions of particles were 5.7 mm in length and 0.38 mm in thickness. Particles were conditioned to 11% moisture content. The adhesive resin used was an isocyanate compound (IC) resin, UL-4800, formulated by Gun-ei Kagaku Kogyo Co. Ltd. The resin content level was ten percent of resin solid based on oven-dry weight of particles. In order to obtain a suitable vicosity of the adhesive for spraying, acetone was added to the IC resin at 20 percent based on weight of the resin solids. The resin was sprayed on the particle in a drum-type rotary blender by means of an airless gun. Hand-formed particle mats were pressed to a board thickness of 20 mm.

In the case of steam-injection pressing, steam was injected for 3 s at mat bulk desnsity of 0.4 g/cm^3 for both the target board densities of 0.4 and 0.6 g/cm^3. The target steam pressure was 6

kgf/cm^2 (about 160°C) with an effective steam pressure of 4 kgf/cm^2 (140°C). The temperature of the hot-platens was set at 160°C with a press pressure of 5 to 10 kgf/cm^2. Total press-time were 30, 45, 60, and 120 s for a board density of 0.4 g/cm^3, and 30, 60, 90, and 120 s for a board density of 0.6 g/cm^3. The total press-time was measured from pressure build-up. In the case of conventional pressing, temperature of platens was set at 160°C. The first stage pressure was set at 15 to 20 kgf/cm^2 for 30 s, and the second stage pressure was set at 5 to 10 kgf/cm^2 for 2.5, 3.5, and 4.5 min which correspond to the total press-time 3, 4 and 5 min. One board of 500×400×20 (t) mm was prepared for each condition mentioned above and for each target density of 0.4 and 0.6 g/cm^3.

Specimens cut from the above were tested after conditioning for 2 weeks at 20°C and 65% relative humidity (RH). Modulus of elasticity (MOE) and modulus of rupture (MOR) in both air-dry and wet conditions, internal bond strength (IB), screw withdrawal resistance (SW) and thickness swelling (TS) were measured according to Japanese Industrial Standard (JIS) A5908.

3.3.2 Results and discussion

The effects of press time on MOE and MOR under dry and wet conditions are shown in Fig. 3.14 and 3.15. The steam-injection pressed boards showed no decrease in MOE and MOR properties both in air-dry and wet conditions for densities level of 0.4 and 0.6 g/cm^3, with reduction of total press time including 3-s-steam-injection down to 30 s and 1 min, respectively. On the other hand, for the conventional pressing, the press-time can be shortened to 3 and 4 min for board densities of 0.4 and 0.6 g/cm^3, respectively. Delamination of board was observed for board density of 0.6 g/cm^3 when press-time were 30 s and 3 min for board produced by steam-

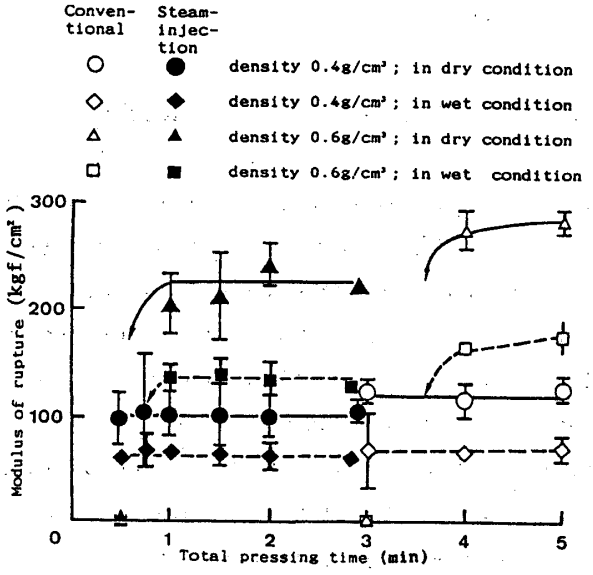

Fig. 3.14. Relationships between total pressing time and modulus of elasticity in dry and wet condition.
Note: The ranges of the mean value show 95% confidence intervals.

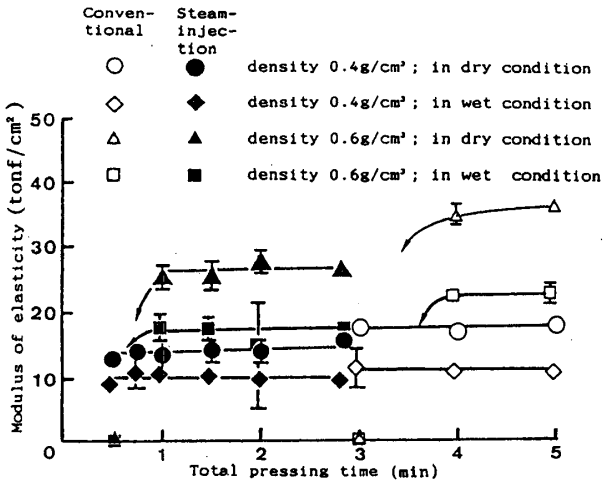

Fig. 3.15. Relationships between total pressing time and modulus of rupture in dry and wet condition.
Note: The ranges of the mean value show 95% confidence intervals.

injection and conventional pressing, respectively. The difference in the minimum press-time with different board densities may be attributed to the difference in internal stress, diffusion resistance during steam-injection and a rising rate of temperature in the core of mats. The values of MOE and MOR were similar to each other for the boards with a density of 0.4 g/cm^3 produced with both pressing systems. However, higher values of MOE and MOR were obtained in conventional pressing than in steam-injection pressing in the case of 0.6 g/cm^3 density board. This may be due to differences on density distribution across board thickness as described in the Section 3.1.2.

The relationship between press-time and IB is shown in Fig. 3.16. For board density of 0.4

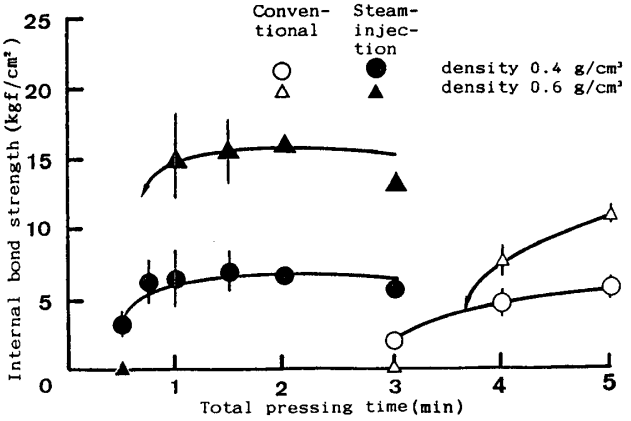

Fig. 3.16. Relationships between total pressing time and internal bond strength.
Note: The ranges of the mean value show 95% confidence intervals.

g/cm^3, though the IB value did not decrease when press-time was shortened to 45 s, it began to decrease at a press-time of 30 s. In the case of 0.6 g/cm^3 board density, the margin of press-time was about 60 s. On the other hand, for both boards with densities of 0.4 and 0.6 g/cm^3 produced by conventional pressing, this corresponded with the temperature behavior in the core of particle mat. The IB expresses the bonding strength of the weakest bonded layers. In other words, it is a direct measure of curing grade of adhesive in the middle layer when reducing press-time. This experimental result suggested that required press-time using steam-injection pressing was 45 and 60 s for board densities of 0.4 and 0.6 g/cm^3, respectively. This corresponds to only 1/5 to 1/6 of

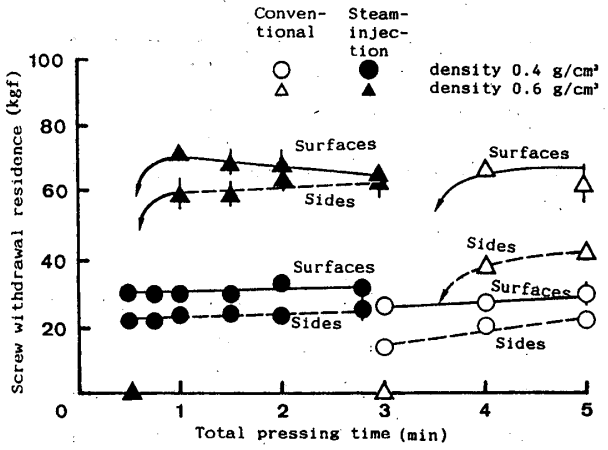

Fig. 3.17. Relationships between total pressing time and screw withdrawal residence.
Note: The ranges of the mean value show 95% confidence intervals.

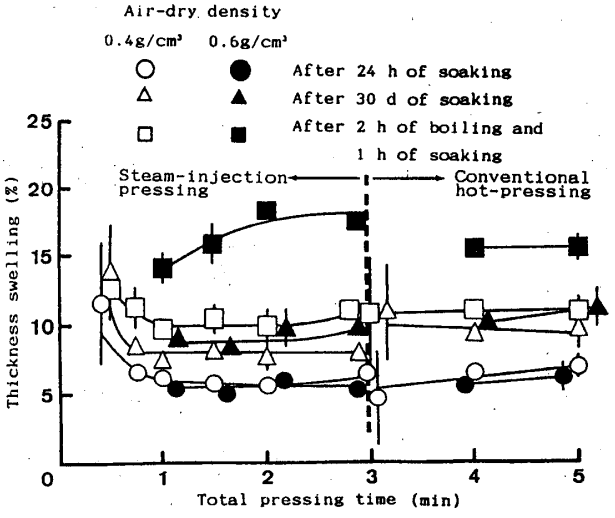

Fig. 3.18. Relationships between total pressing time and thickness swelling.
Note: The ranges of the mean value show 95% confidence intervals.

the press-time necessary for the conventional pressing. The results of this experiment agree well with the results obtained in the foregoing chapter concerning curing condition of particleboard adhesive using isocyanate resin[27].

The relationships between SW, TS properties and press time are shown in Figures 3.17 and 3.18, respectively. The results were similar with those obtained in IB test mentioned above.

3.4 Summary

First, the effect of steam-injection time and timing on the physical properties of particleboard was examined to get the optimum conditions for steam-injection pressing. Owing to the the difference of the density distribution through the board thickness, the flexure properties of the greater density boards made with steam-injection pressing had values a little smaller than those made with conventional hot-platen pressing and their dimensional stability under wet conditions also tended to increase. The board properties were almost independent of the steam-injection time. The bending properties tended to increase with the delay of the initiation of the steam injection in most dense particleboards. This means that sufficient contact between particles before steam injection was best. In spite of the above results, initiation of the steam injection at the compaction ratio of 1.0 to 1.3 would be rational for shortening the total press time because a longer pressing time and a greater pressure were needed to compress the mats to a target density in the production of boards of greater densities.

Secondly, each of seven types of Japanese red pine particles with different dimensions, strictly controlled for length, width, and thickness, was prepared in order to produce particle boards with a density range of 0.3–0.6 g/cm^3 under different pressing conditions. Mechanical and physical properties of these boards were determined and the effect of particle geometry and pressing conditions were discussed. It revealed that particle geometry influenced the way how steam diffuses into the mat. Based on the experiments conducted, it can be surmised that both steam diffusion and particle geometry have correlation on the properties of the final products.

Finally, the minimum and necessary press-time of steam-injection pressed, particleboards with a thickness of 20 mm using an adhesive and the effect of total press-time on the particleboard properties were investigated. Steam-injection pressing made it possible to produce particleboards in only 1/5–1/6 of the press time of conventional hot-platen pressing.

Conclusion

This paper is written in three chapters with the aim of establishing the basic theories of the steam-injection pressing which is the most effective technology to improve the productivity of the wood-composite-products, while the effective utilization of low-quality wood resources is kept in mind.

First, the temperature behavior of the particle mat during hotpressing and steam-injection pressing was analyzed under various conditions in Chapter 1. With an increase of

moisture content, the time necessary for the middle layer to reach 100°C tended to shorten, whereas the time to maintain a constant temperature (about 100°C) was prolonged in the case of hotpressing. The temperature in the middle layer of a mat with a higher moisture content in the face layers increased more than that of a mat with a uniform distribution of moisture content. In the case of steam-injection pressing, the temperature in the middle layer of the mats immediately increased to a specific degree decided by injection pressure and the characteristics of mats at the moment of steam-injection, and maintained a constant level during steam-injection. After stopping steam-injection, the temperature decreased a little, and then started to rise again. The rates of temperature increase in the middle layers of mats were independent of thickness, moisture content and density in the range of the experimental conditions.

Secondly, the temperature distribution in particle mats during steam-injection pressing was numerically analyzed with the finite element method under various conditions in this Chapter. Calculated results agreed comparatively well with the observed results, which proved that the analytical theory was useful to predict the temperature behavior of particle mats during hotpressing and steam-injection pressing. In steam-injection pressing, with increases of mat thickness, the injection time necessary for raising core temperature up to 100°C gradually increased. For example, it will take about 8 s for the core temperature of a 1000-cm-thick mat, to reach 100°C.

The temperature behavior in the mat and the air permeability of the boards were investigated in Chapter 2, using each of seven types of particles with different dimensions, strictly controlled for length, width, and thickness. The variables influencing the temperature behavior in the mat by steam-injection press was directly related to the air permeabilities of mats. The air permeabilities of the boards in the horizontal direction to the heat platen was always higher than in the vertical direction. A functional equation with a higher coefficient of determination that explains the air permeabilities was obtained by a multiple regression analysis. It was inferred that the steam diffusion in the mat result from the repetition of the steam moving among particles in two dimensions.

First, the effects of injection time and injection timing of high-pressure steam from hot platens on the physical properties of particleboards using an isocyanate-compound adhesives were investigated and the optimum conditions for steam-injection pressing was determined in Chapter 3. Owing to the difference of the density distribution through the board thickness the flexure properties of the greater density boards made with steam-injection pressing had values a little smaller than those made with conventional hot-platen pressing and their dimensional stability under wet conditions also tended to increase. The board properties were almost independent of the steam-injection time. The bending properties tended to increase with the delay of the initiation of the steam injection in most dense particleboards. This means that sufficient contact between particles before steam

injection was best. In spite of the above results, initiation of the steam injection at the compaction ratio of 1.0 to 1.3 would be rational for shortening the total press time because a longer pressing time and a greater pressure were needed to compress the mats to a target density in the production of boards of greater densities.

Secondly, this chapter showed the experiment where each of seven types of Japanese red pine particles with different dimensions, strictly controlled for length, width, and thickness, was prepared in order to produce particleboards under different pressing conditions, mechanical and physical properties of these boards were determined, and the effect of particle geometry and pressing conditions were discussed. It revealed that particle geometry influenced the way how steam diffuses into the mat. Based on the experiments conducted, it can be surmised that both steam diffusion and particle geometry have correlation on the properties of the final products.

Thirdly, the effects of pressing time on the physical properties were investigated in this chapter to find the minimum press time required to produce particleboards using an isocyanate-compound adhesive with the steam-injection pressing. Steam-injection pressing made it possible to produce particleboards in only 1/5–1/6 of the press time of conventional hot-platen pressing.

As mentioned above, it shows in the first part of this study that the steam-injection pressing fulfilled the requirements for lower density or thicker boards. The temperature behavior of particle mats during pressing was then investigated from the experiments and the computer simulation. It was made clear that this technology made it possible to produce boards with excellent properties and will improve productivity. The results of the experiment on the effects of particle geometry on air permeabilities will offer useful information in the development of a full scale continuous steam-injection press as well as the potential of the applied process of the steam-injection pressing in the production of wood composite products.

It follows from what has been said that this study would give us a deeper significance because the purpose of this research is the effective utilization of lower quality wood and the effective production of value-added functional materials with saved energy in order to face the inadequate supply of wood and its subsequent adverse effect on wood quality.

In relation to this study, many interesting subjects are still left and these are as follows: The development of new and thick wood composite products; The development of a full scale continuous steam-injection press; A study on the improvement of the dimensional stability and endurance of the products; and a study of the board production with applied technology of the steam-injection pressing; and so on.

Acknowledgement

I would like to express gratitude for the privilege of being able to study under Professor Dr. Hikaru Sasaki, Wood Research Institute, Kyoto University, and for his invaluable supervision. I would also like to thank Professor Dr. Takeshi Sadoh, Faculty of Agriculture, Kyoto University, and to Professor Dr. Misato Norimoto, Wood Research Institute, Kyoto University, as co-supervisor.

Special thanks are due to Associate Professor Dr. Shuichi Kawai, Wood Research Institute, Kyoto University, for reading the manuscript and making a number of helpful suggestions. I would also like to thank Professor Dr. Shigehisa Ishihara, Associate Professor Dr. Yuji Imamura and Instructor Mr. Shinjiro Takino of the above Institute for their constant support and instructions. My further thanks are extended to Dr. Toru Ebihara, Forestry and Forest Products Research Institute, Ministry of Agriculture, Forestry and Fishries, for his help and suggestions on some parts of this research.

I would also like to acknowledge the invaluable support of Mr. Hisayoshi Suda, Sumitomo Ringyo Co. Ltd., Mr. Divino. E. Teixeria, Laboratorio De Productos Florestais, Bambang Subiyanto, Research and development Center for Applied Physics. Mr. Nakano Masashi, Iwate Prefectural Forestry and Forest Products Research Center, Mr. Yoki Suzuki, Forestry and Forest Products Research Institute, and Mrs. Hiromi Hata. Thanks must also be extended to members in the Research Section of Composite Wood and in the Forestry and Forest Products Research Institute for their help and encouragement; in particular to Dr. Orlando R. Pulido and Mr. Dweight A. Eusebio for his critical reading this manuscript.

References

1) S. KAWAI and T. HATA: *Wood Industry,* **42**(12), 562–565 (1987).
2) R.L. GEIMER: Proc. Wash. State Univ. Int. Symp. Part. 16, 115–134 (1982).
3) M. NAKAJI, S. KAWAI and S. MORITA: *Wood Preservation,* **26**, 53–59 (1985).
4) B. GRETEN: *Holz als Roh- und Werkstoff,* **44**, 371–378 (1986).
5) H. SOIN: *Holz als Roh- und Werkstoff,* **42**, 63–66 (1984).
6) H. SOIN: *Holz als Roh- und Werkstoff,* **42**, 93–98 (1984).
7) H. SOIN: *Holz als Roh- und Werkstoff,* **44**, 371–378 (1986).
8) W. WILLIAMS: Wood Based Panels North America, 2, 25–27, (1989).
9) H.J. DEPPE and K. ERNST: *Holz als Roh- und Werkstoff,* **29**(2) 45–50 (1971).
10) E. ROFFAEL and W. Rauch: *Holz als Roh- und Werkstoff,* **31**(10), 402–405 (1973).
11) W.E. JOHNS, T.M. MALONY, E.M. HUFFAKER, J.B. SAUNDERS and M.T. LENTZ: Proc. Wash. State Univ Int. Symp. Part. 15, 213–239 (1981).
12) S. KAWAI, H. SASAKI and M. NAKAJI: *Wood Research,* **72**, 27–36 (1986).
13) S. KAWAI and H. SASAKI: *Mokuzai Gakkaishi,* **32**(5), 324–330 (1986).
14) Y. YOSHIDA, et al.: *Mokuzai Gakkaishi,* **32**(12), 965–971 (1986).
15) T. MAKU: *Mokuzai Kenkyu,* **3**, 1–36 (1949).
16) T. MAKU and N. MATSUURA: *Mokuzai Kenkyu,* **3**, 37–53 (1949).
17) T. HATA, Subiyanto BAMBANG, S. KAWAI and H. SASAKI: *Wood Sci. Technol,* **23**, 361–369, 12 (1989).

18) K.C. SHEN : *Forest Prod. J.*, **23**(3), 21–29 (1973).
19) T. MAKU, R. HAMADA and H. SASAKI : *Wood Research*, **21**, 47–50 (1959).
20) T. MAKU, R. HAMADA and H. SASAKI : *Mokuzai Kenkyu*, **21**(11), 34–46 (1958).
21) T. HATA, S. KAWAI and H. SASAKI : *Wood Sci. Technol*, **24**, 65–78 (1990).
22) G. YAGAWA and N. MIYAZAKI : Analysis of Thermal Stress, Creep and Thermal Conduction by Finite Element Method, Science Co. (1985).
23) G.S. CANBELL : Soil Physics with Basic-Transport Models for soil-systems, Elsevier Science Publishing Company Inc. 40 (1985).
24) T. HATA, et al. : *Mokuzai Gakkaishi*, **39**(2), 161–168 (1993).
25) T. HATA, et al. : *Mokuzai Gakkaishi*, **39**(2), 169–173 (1993).
26) T. OGURA : *Bulletin of Forestry ajd Forest Products Research Institute*, **51**, 61–75 (1951).
27) Subiyanto BAMBANG, S. KAWAI, H. SASAKI, N. KAHAR and H. SHIGEHIRA, : *Mokuzai Gakkaishi*, **34**(4), 333–336 (1988).
28) L.P. FUTO : *Holz als Roh- und Werkstoff*, **28**(11), (1970).
29) Y. SUZUKI,T. HAISHI and H.SAITO : Abst. 39th Annu. Meet. Jpn. Wood Res. Soc., Okinawa, p. 16 (1989).
30) T. OKUNO, H. KUME and H. SAITO : "Multivariate Analysis", Nikkagiren, 141 (1989).
31) T. HATA, Subiyanto BAMBANG and H. SASAKI : *Mokuzai Gakkaishi*, **35**(12), 1080–1086 (1989).
32) W.E. HSU : Spring Meeting, Eastern Canadian Section, For. Prod. Res. Soc. (1990).
33) T. HATA, S. KAWAI and H. SASAKI : *Mokuzai Gakkaishi*, **35**(12), 1087–1091 (1989).